Wave resonances and coupled-mode equations for three-dimensional photonic crystals

Dmitry Pelinovsky
Department of Mathematics, McMaster University,
1280 Main Street West, Hamilton, Ontario, Canada, L8S 4K1

March 30, 2004

Abstract

Coupled-mode equations are derived for modelling of low-contrast weakly nonlinear photonic crystals in three spatial dimensions. Coupled-mode equations correspond to normal forms for Bragg resonances of Bloch waves in photonic stop bands. Lower-order Bragg resonances are classified in a cubic crystal lattice, and two-wave and four-wave equations are derived explicitly from the nonlinear Maxwell equations. The boundary-value problem for stationary transmission of the resonant waves is studied analytically within the linear coupled-mode equations. Using the method of separation of variables and generalized Fourier series, integral invariants for transmission, reflection and diffraction of resonant waves are computed from analytical solutions of the stationary transmission problem.

1 Introduction

Photonic band-gap crystals are periodic optical materials, spectrum of which consists of bands, separated by band gaps [12]. Periodic and nonlinear properties of the photonic crystals are modelled with the nonlinear Maxwell equations:

$$\nabla^2 \mathbf{E} - \frac{n^2}{c^2} \frac{\partial^2 \mathbf{E}}{\partial t^2} = \nabla \left(\nabla \cdot \mathbf{E} \right), \qquad \nabla \cdot \left(n^2 \mathbf{E} \right) = 0, \tag{1.1}$$

where $n = n(\mathbf{x}, |\mathbf{E}|^2)$ is the refractive index, $\mathbf{E} = (E_x, E_y, E_z)$ is the complex-valued electric field, $\mathbf{x} = (x, y, z)$ is the physical space, t is the time variable, $\nabla = (\partial_x, \partial_y, \partial_z)$ is the gradient vector, and c is the speed of light. Components of the magnetic field are eliminated from the vector Maxwell equations (1.1) [12].

In one dimension, the nonlinear Maxwell equations (1.1) can be simplified for a linearly polarized light, such that $\mathbf{E} = (E, 0, 0)$, $E = E(z, t)$, and $n = n(z, |E|^2)$, . The scalar component $E(z, t)$ solves the nonlinear wave equation:

$$\frac{\partial^2 E}{\partial z^2} - \frac{n^2(z, |E|^2)}{c^2} \frac{\partial^2 E}{\partial t^2} = 0. \tag{1.2}$$

If the linear refractive index $n_0(z) = n(z,0)$ is a periodic function with period z_0, the linear spectrum of (1.2) reduces to the Matthew-type equation for $E(z,t) = \psi(z)e^{-i\omega t}$, where ω is the eigenvalue and $\psi(z)$ is the eigenfunction of the spectral problem:

$$\psi'' + \frac{\omega^2}{c^2} n_0^2(z)\psi = 0. \tag{1.3}$$

According to the Floquet theory [11], solutions of the Matthew equation (1.3) take the form: $\psi(z) = \Psi(z)e^{ik(\omega)z}$, where $\Psi(z+z_0) = \Psi(z)$ and $k = k(\omega)$ is the propagation constant. For a general class of periodic potentials $n_0^2(z)$, there exist infinitely many intervals of ω, called band gaps, where the propagation constant $k(\omega)$ is purely imaginary and the Bloch function $\psi(z)$ is unbounded in z. The band gaps are supported by the low-contrast photonic crystal, when $n_0(z) = n_0 + \epsilon n_1(z)$, where n_0 is constant and ϵ is small parameter.

In two and three dimensions, the linear Maxwell equations (1.1) with $n_0(\mathbf{x}) = n(\mathbf{x},0)$ can also be reduced to a spectral problem for $\mathbf{E}(\mathbf{x},t) = \boldsymbol{\psi}(\mathbf{x})e^{-i\omega t}$, where ω is the eigenvalue and $\boldsymbol{\psi}(\mathbf{x})$ is the eigenvector. When $n_0(\mathbf{x})$ is a periodic function in x, y, z with periods x_0, y_0, z_0, respectively, the eigenvector $\boldsymbol{\psi}(\mathbf{x})$ satisfies the Floquet theorem [11] and has the form of the Bloch wave: $\boldsymbol{\psi}(\mathbf{x}) = \boldsymbol{\Psi}(\mathbf{x})e^{i(k_x x + k_y y + k_z z)}$, where $\boldsymbol{\Psi}(\mathbf{x})$ is periodic in x, y, and z with periods x_0, y_0, and z_0, and $\omega = \omega(k_x, k_y, k_z)$. No band gaps exist in the linear spectrum for low-contrast photonic crystals. As a result, the bounded Bloch functions $\boldsymbol{\psi}(\mathbf{x})$ may exist for any value of $\omega \in \mathbb{R}$. Highly-contrast photonic crystals may however exhibit band gaps for some configurations of the linear refractive index $n_0^2(\mathbf{x})$ [12].

When weak Kerr cubic nonlinearity is taken into account in the photonic band-gap crystals, the refractive index $n(\mathbf{x}, |\mathbf{E}|^2)$ is decomposed into the linear and nonlinear parts:

$$n(\mathbf{x}, |\mathbf{E}|^2) = n_0(\mathbf{x}) + \epsilon n_2(\mathbf{x})|\mathbf{E}|^2, \tag{1.4}$$

where ϵ is small parameter. The Cauchy problem for the nonlinear wave equation (1.2) and nonlinear Maxwell equations (1.1) with $n_2(\mathbf{x}) \neq 0$ is generally not well-posed for all $0 \leq t < \infty$ since shock wave singularities may occur in finite time $t = t_* < \infty$ [8]. Therefore, nonlinear Maxwell equations with refractive index $n(\mathbf{x}, |\mathbf{E}|^2)$ must be modified, in order to exclude formation of shock wave singularities and to ensure that the Cauchy problem is globally well-posed. One modification is based on the account of dispersive terms $n(\mathbf{x}, |\mathbf{E}|^2, \omega)$ in modelling of time-dependent responses of nonlinear photonic crystals [4, 5]. Another modification is based on the reduction of nonlinear Maxwell equations to the coupled-mode equations [8, 21].

Coupled-mode equations are typically derived in the first band gap of the Bragg resonance between two counter-propagating waves in one spatial dimension [18, 19]. More complicated coupled-mode equations are recently considered for three-dimensional nonlinear photonic crystals [1, 2, 3, 6]. Recent reviews [4, 5] include also classification of different resonances of Bloch waves in photonic crystals with quadratic nonlinearities.

In this paper, a classification of wave resonances and coupled-mode equations is considered for low-contrast, weakly nonlinear photonic crystals in three spatial dimensions. Since low-contrast

crystals do not support band gaps beyond one dimension [11, 12], resonances are considered in stop bands of the linear spectrum, according to standard definitions of solid state physics [10]. Stop bands occur between resonant counter-propagating waves, which could be coupled resonantly with other oblique Bloch waves.

Lowest-order Bragg resonances in the stop bands of the linear spectrum are classified here in the context of cubic lattice crystals. The number of resonant Bloch waves depends on the geometric configuration of the incident wave with respect to the cubic lattice. When the nonlinear Maxwell equations are truncated at the normal forms with the perturbation series expansions, coupled-mode equations for the lowest-order Bragg resonances are derived and studied in bounded domains, subject to the radiation boundary conditions.

The linear coupled-mode equations for two and four resonant Bloch waves are studied here with the method of separation of variables and generalized Fourier series [22]. Although the linear operators are not self-adjoint due to the radiation boundary conditions, convergence of generalized Fourier series follows from the general theory [7]. As a result, explicit analytical expressions for stationary transmission, reflection, and diffraction of two and four resonant Bloch waves are obtained here from the Fourier series solutions.

The paper is organized as follows. Classification of resonances in cubic lattice crystals is given in Section 2. Systematic derivation of coupled-mode equations for lowest-order resonances of two and four Bloch waves is described in Section 3. Analysis of boundary-value problems for stationary transmission of resonant Bloch waves is reported in Section 4, within the linear coupled-mode equations. Section 5 concludes the paper.

2 Classification of resonances

When the optical material is homogeneous, such that $n_0(\mathbf{x}) = n_0$, where n_0 is constant, the linear spectrum of the Maxwell equations (1.1) is defined by the free transverse waves,

$$\mathbf{E}(\mathbf{x}, t) = \mathbf{e}_{\mathbf{k}} e^{i(\mathbf{k}\cdot\mathbf{x} - \omega t)}, \tag{2.1}$$

where $\mathbf{e}_{\mathbf{k}}$ is the polarization vector, $\mathbf{k} = (k_x, k_y, k_z)$ is the wavevector, and $\omega = \omega(\mathbf{k})$ is the wave frequency. It follows from the system (1.1) that

$$\mathbf{k} \cdot \mathbf{e}_{\mathbf{k}} = 0, \qquad \omega^2 = \frac{c^2}{n_0^2} \left(k_x^2 + k_y^2 + k_z^2 \right). \tag{2.2}$$

For each wavevector $\mathbf{k}$, there exist two independent polarizations $\mathbf{e}_{\mathbf{k}}^{(1)}$ and $\mathbf{e}_{\mathbf{k}}^{(2)}$, such that $\mathbf{e}_{\mathbf{k}}^{(1)} \cdot \mathbf{e}_{\mathbf{k}}^{(2)} = 0$. This degeneracy in the polarization vector is neglected here by the assumption that the incident wave is linearly polarized.

The incident wave vector $\mathbf{k}_{\text{in}}$ can be parameterized in the spherical coordinates:

$$\mathbf{k}_{\text{in}} = k \left(\sin\theta \cos\varphi, \sin\theta \sin\varphi, \cos\theta \right), \qquad k \in \mathbb{R}, \quad 0 \leq \theta \leq \pi, \quad 0 \leq \varphi \leq 2\pi, \tag{2.3}$$

where $k = |\mathbf{k}_{\text{in}}|$ is the wave number of the incident wave and (θ, φ) are latitude and polar angles with respect to the photonic crystal. The case $\theta = 0$ corresponds to the propagation of the incident wave in the z-direction.

When the optical material is low-contrast, such that

$$n_0(\mathbf{x}) = n_0 + \epsilon n_1(\mathbf{x}), \tag{2.4}$$

where ϵ is small parameter, the incident wave interacts with the photonic crystal due to the interference term $n_1(\mathbf{x})\mathbf{E}(\mathbf{x}, t)$ in the Maxwell equations (1.1). The geometric configuration of the photonic crystal is defined by the fundamental (linearly independent) lattice vectors $\mathbf{x}_{1,2,3}$ and fundamental reciprocal lattice vectors $\mathbf{k}_{1,2,3}$, such that $\mathbf{k}_i \cdot \mathbf{x}_j = 2\pi\delta_{i,j}$, where $1 \leq i, j \leq 3$ [10]. Therefore, the linear refractive index $n_1(\mathbf{x})$ can be expanded into triple Fourier series:

$$n_1(\mathbf{x}) = n_0 \sum_{(n,m,l)\in\mathbb{Z}^3} \alpha_{n,m,l} e^{i(n\mathbf{k}_1 + m\mathbf{k}_2 + l\mathbf{k}_3)\cdot\mathbf{x}}, \tag{2.5}$$

where the factor n_0 is introduced for convenience. The incident wave with the wave vector $\mathbf{k}_{\text{in}}$ generates an infinite number of scattered waves with the wave vectors $\mathbf{k}_{\text{out}}^{(n,m,l)}$:

$$\mathbf{k}_{\text{out}}^{(n,m,l)} = \mathbf{k}_{\text{in}} + n\mathbf{k}_1 + m\mathbf{k}_2 + l\mathbf{k}_3, \qquad (n, m, l) \in \mathbb{Z}^3. \tag{2.6}$$

Definition 2.1 *The wave vector $\mathbf{k}_{\text{out}}^{(n,m,l)}$ with a non-empty triple (n, m, l) is said to be resonant with the wave vector $\mathbf{k}_{\text{in}}$, if $|\mathbf{k}_{\text{out}}^{(n,m,l)}| = |\mathbf{k}_{\text{in}}| = k$, such that $|\omega(\mathbf{k}_{\text{out}}^{(n,m,l)})| = |\omega(\mathbf{k}_{\text{in}})|$.*

The wave resonances are classified here for a simple cubic crystal when the fundamental lattice vectors and reciprocal lattice vectors are all orthogonal [10]:

$$\mathbf{x}_{1,2,3} = a\mathbf{e}_{1,2,3}, \qquad \mathbf{k}_{1,2,3} = k_0\mathbf{e}_{1,2,3}, \qquad k_0 = \frac{2\pi}{a}, \tag{2.7}$$

where $\mathbf{e}_{1,2,3}$ are unit vectors in $\mathbb{R}^3$. The coordinate axes (x, y, z) are oriented along the axes of the simple cubic crystal, while the incident wave vector $\mathbf{k}_{\text{in}}$ is directed according to the spherical angles (θ, φ) in (2.3). When $\theta = 0$, the wave vector $\mathbf{k}_{\text{in}}$ is perpendicular to the (x, y) crystal plane. For the simple wave crystal, the set of resonant Bloch waves is given by the set of triples:

$$\mathcal{S} = \{(n, m, l) \in \mathbb{Z}^3 : \ n(n + p) + m(m + q) + l(l + r) = 0, \ |n| + |m| + |l| \neq 0\}, \tag{2.8}$$

where

$$p = \frac{2k}{k_0}\sin\theta\cos\varphi, \quad q = \frac{2k}{k_0}\sin\theta\sin\varphi, \quad r = \frac{2k}{k_0}\cos\theta \tag{2.9}$$

are given real-valued parameters. The set of parameters (p, q, r) is given by the geometric orientation of the incident wave vector $\mathbf{k}_{\text{in}}$ with respect to the cubic lattice crystal.

Lemma 2.2 *When $(p, q, r) \in \mathbb{Z}^3$ and $|p| + |q| + |r| \neq 0$, the set $\mathcal{S}$ is non-empty.*

Proof. There exists at least one non-zero resonant triple: $(n, m, l) = (-p, -q, -r)$. ∎

When $(p,q,r) \in \mathbb{Z}^3$, resonant triples (n,m,l) can be all classified analytically. However, when $(p,q,r) \notin \mathbb{Z}^3$, additional resonant triples may also exist. In solid state physics [10], a geometric solution for the resonant triples (n,m,l) is constructed from the condition that the vector $\mathbf{G}^{(n,m,l)} = \mathbf{k}_{\mathbf{out}}^{(n,m,l)} - \mathbf{k}_{\mathbf{in}}$ lies on the edge of the Brillouin zone of the photonic crystal lattice. Here we review particular resonant sets $\mathcal{S}$ for integer and non-integer values of (p,q,r).

2.1 Family of one-dimensional resonances

The one-dimensional Bragg resonance occurs when the incident wave is coupled with the counter-propagating reflected wave, such that the set $\mathcal{S}$ is non-empty: $\mathcal{S} = \{(0,0,-r)\}$, where $r \in \mathbb{N}_+$. The values of p and q are not defined for the Bragg resonance, when $n = m = 0$. As a result, spherical angles θ and φ in the parametrization (2.3) are arbitrary, while the wave number k satisfies the Bragg resonance condition [10]:

$$rk_0 = 2k\cos\theta, \tag{2.10}$$

such that $r\lambda = 2a\cos\theta$, where λ is the wavelength.

The one-dimensional Bragg resonance is generalized in three dimensions for $p = q = 0$ and $r \in \mathbb{N}_+$, when the geometric configuration for the Bragg resonance (2.10) is fixed at the specific value $\theta = 0$, and

$$\mathbf{k}_{\mathbf{in}} = \frac{\pi}{a}(0,0,r), \qquad \mathbf{k}_{\mathbf{out}}^{(0,0,-r)} = \frac{\pi}{a}(0,0,-r). \tag{2.11}$$

The incident wave is directed to the z-axis of the cubic lattice crystal and the wavelength is $\lambda = 2a/r$. The family of Bragg resonances with $p = q = 0$ and $r \in \mathbb{N}_+$, may include not only the two counter-propagating waves (2.11) but also other Bloch waves in three-dimensional photonic crystals. The lowest-order resonant sets $\mathcal{S}$ for $p = q = 0$ and $r \in \mathbb{N}_+$ are listed below:

$r = 1$: $\mathcal{S} = \{(0,0,-1)\}$

$r = 2$: $\mathcal{S} = \{(1,0,-1),(-1,0,-1),(0,1,-1),(0,-1,-1),(0,0,-2)\}$

$r = 3$: $\mathcal{S} = \{(1,1,-1),(-1,1,-1),(1,-1,-1),(-1,-1,-1),(1,1,-2),(-1,1,-2),(1,-1,-2)\} \cup$
$\{(-1,-1,-2),(0,0,-3)\}$

The dimension of $\mathcal{S}$ depends on the total number of all possible integer solutions for (n,m,l). The sets $\mathcal{S}$ for higher-order resonances with $r \in \mathbb{N}_+$ can be found algorithmically, with the symbolic computing software.

2.2 Families of two-dimensional resonances

Two-dimensional Bragg resonances occur when the incident wave vector $\mathbf{k}_{\mathbf{in}}$ is resonant to the counter-propagating reflected wave vector $\mathbf{k}_{\mathbf{out}}^{(-p,-q,0)}$, as well as to two other diffracted wave vectors $\mathbf{k}_{\mathbf{out}}^{(0,-q,0)}$ and $\mathbf{k}_{\mathbf{out}}^{(-p,0,0)}$, where $(p,q) \in \mathbb{N}_+^2$. The value of r is not defined for the two-dimensional resonance, such that the angle θ in the parametrization (2.3) is arbitrary, while k

and φ satisfy the resonance conditions:

$$\varphi = \arctan\left(\frac{q}{p}\right), \qquad \sqrt{p^2+q^2}k_0 = 2k\sin\theta. \tag{2.12}$$

The two-dimensional Bragg resonances are generalized in three dimensions for $(p,q) \in \mathbb{N}_+^2$ and $r=0$, when the geometric configuration for the Bragg resonance (2.12) is fixed at the specific value $\theta = \frac{\pi}{2}$, and

$$\begin{aligned} \mathbf{k}_{\rm in} &= \frac{\pi}{a}(p,q,0), \qquad \mathbf{k}_{\rm out}^{(-p,-q,0)} = \frac{\pi}{a}(-p,-q,0), \\ \mathbf{k}_{\rm out}^{(0,-q,0)} &= \frac{\pi}{a}(p,-q,0), \qquad \mathbf{k}_{\rm out}^{(-p,0,0)} = \frac{\pi}{a}(-p,q,0). \end{aligned} \tag{2.13}$$

The incident wave $\mathbf{k}_{\rm in}$ is directed alone the diagonal of the (px,qy)-cell of the cubic lattice crystal and the wavelength is $\lambda = 2a/\sqrt{p^2+q^2}$.

The families of Bragg resonances with $(p,q) \in \mathbb{N}_+^2$ and $r=0$ may include not only the four resonant waves (2.13) but also other Bloch waves in three-dimensional photonic crystals. The lowest-order resonant sets $\mathcal{S}$ for $(p,q) \in \mathbb{N}_+^2$ and $r=0$ are listed below:

$p=1, q=1$: $\mathcal{S} = \{(-1,0,0),(0,-1,0),(-1,-1,0)\}$

$p=2, q=1$: $\mathcal{S} = \{(0,-1,0),(-1,0,1),(-1,0,-1),(-1,-1,1),(-1,-1,-1),(-2,0,0),(-2,-1,0)\}$

$p=2, q=2$: $\mathcal{S} = \{(0,-1,1),(0,-1,-1),(0,-2,0),(-1,0,1),(-1,0,-1),(-1,-2,1)\} \cup$
$\{(-1,-2,-1),(-2,0,0),(-2,-1,1),(-2,-1,-1),(-2,-2,0)\}$

Additional two-dimensional resonances are described by the resonant sets:

$$\mathcal{S}_{2D} = \left\{(n,m) \in \mathbb{Z}^2 : \; n(n+p)+m(m+q) = 0, \; |n|+|m| \neq 0\right\}, \tag{2.14}$$

when either $p \notin \mathbb{Z}$ or $q \notin \mathbb{Z}$ or both. In particular, there exists a possibility of the resonance between the incident and diffracted waves, which are not generally parallel to each other:

$$\mathbf{k}_{\rm in} = \frac{\pi}{a}(p,q,0), \qquad \mathbf{k}_{\rm out}^{(n,m,0)} = \frac{\pi}{a}(p+2n, q+2m, 0). \tag{2.15}$$

The resonance condition (2.14) leads to the only constraint on $(p,q) \in \mathbb{R}^2$:

$$np + mq = -(n^2+m^2). \tag{2.16}$$

Similarly, resonance of three oblique waves is also possible on the (x,y)-plane:

$$\mathbf{k}_{\rm in} = \frac{\pi}{a}(p,q,0), \;\; \mathbf{k}_{\rm out}^{(n_1,m_1,0)} = \frac{\pi}{a}(p+2n_1, q+2m_1, 0), \;\; \mathbf{k}_{\rm out}^{(n_2,m_2,0)} = \frac{\pi}{a}(p+2n_2, q+2m_2, 0), \tag{2.17}$$

where $m_1 n_2 \neq m_2 n_1$, while (p,q) take rational values:

$$p = \frac{m_1(n_2^2+m_2^2) - m_2(n_1^2+m_1^2)}{m_2 n_1 - m_1 n_2}, \qquad q = \frac{n_1(n_2^2+m_2^2) - n_2(n_1^2+m_1^2)}{n_2 m_1 - n_1 m_2}. \tag{2.18}$$

In general case, two oblique waves (2.15) or three oblique waves (2.17) may have resonances with other Bloch waves in three-dimensional photonic crystals.

2.3 Fully three-dimensional resonances

When $(p,q,r) \in \mathbb{N}_+^3$, the resonant sets $\mathcal{S}$ include eight coupled waves for fully three-dimensional Bragg resonance:

$$\begin{aligned}
\mathbf{k}_{\rm in} &= \frac{\pi}{a}(p,q,r), \qquad \mathbf{k}_{\rm out}^{(-p,-q,-r)} = \frac{\pi}{a}(-p,-q,-r),\\
\mathbf{k}_{\rm out}^{(-p,0,0)} &= \frac{\pi}{a}(-p,q,r), \qquad \mathbf{k}_{\rm out}^{(0,-q,0)} = \frac{\pi}{a}(p,-q,r),\\
\mathbf{k}_{\rm out}^{(0,0,-r)} &= \frac{\pi}{a}(p,q,-r), \qquad \mathbf{k}_{\rm out}^{(-p,-q,0)} = \frac{\pi}{a}(-p,-q,r),\\
\mathbf{k}_{\rm out}^{(-p,0,-r)} &= \frac{\pi}{a}(-p,q,-r), \qquad \mathbf{k}_{\rm out}^{(0,-q,-r)} = \frac{\pi}{a}(p,-q,-r).
\end{aligned} \tag{2.19}$$

The resonance condition for the three-dimensional Bragg resonance takes the form:

$$\varphi = \arctan\left(\frac{q}{p}\right), \qquad \theta = \arctan\left(\frac{\sqrt{p^2+q^2}}{r}\right), \qquad \sqrt{p^2+q^2+r^2}k_0 = 2k, \tag{2.20}$$

The incident wave $\mathbf{k}_{\rm in}$ is directed alone the diagonal of the (px, qy, rz)-cell of the cubic lattice crystal and the wavelength is $\lambda = 2a/\sqrt{p^2+q^2+r^2}$. The eight waves (2.19) can be coupled with some other resonant waves, such that $\dim(\mathcal{S}) \geq 7$ for $(p,q,r) \in \mathbb{N}^3$. For instance, $\dim(\mathcal{S}) = 7$ for $(p,q,r) = (1,1,1)$ and $(p,q,r) = (2,1,1)$, but $\dim(\mathcal{S}) = 9$ for $(p,q,r) = (2,2,1)$ and $\dim(\mathcal{S}) = 15$ for $(p,q,r) = (3,2,1)$.

3 Derivation of coupled-mode equations

The coupled-mode equations are derived for low-contrast and weakly nonlinear photonic crystals, when the refractive index $n(\mathbf{x}, |\mathbf{E}|^2)$ is given by (1.4) and (2.4), such that

$$n(\mathbf{x}, |\mathbf{E}|^2) = n_0 + \epsilon n_1(\mathbf{x}) + \epsilon n_2(\mathbf{x})|\mathbf{E}|^2. \tag{3.1}$$

The small parameter ϵ determines the formal asymptotic solution of the nonlinear Maxwell equations (1.1) in the perturbation series expansions:

$$\mathbf{E}(\mathbf{x},t) = \mathbf{E}_0(\mathbf{x},t) + \sum_{k=1}^{\infty} \epsilon^k \mathbf{E}_k(\mathbf{x},t). \tag{3.2}$$

Assuming that $\dim(\mathcal{S}) < \infty$ in the resonant set (2.8), we set the leading-order term $\mathbf{E}_0(\mathbf{x},t)$ to be a linear superposition of N resonant waves with wave vectors $\mathbf{k}_j$ at the same frequency $\omega = \omega(\mathbf{k}_j)$:

$$\mathbf{E}_0(\mathbf{x},t) = \sum_{j=1}^{N} A_j(\mathbf{X},T)\mathbf{e}_{\mathbf{k}_j} e^{i(\mathbf{k}_j\mathbf{x}-\omega t)}, \qquad \mathbf{X} = \frac{\epsilon \mathbf{x}}{k}, \quad T = \frac{\epsilon t}{\omega}, \tag{3.3}$$

where $A_j(\mathbf{X},T)$ is the envelope amplitude of the $j^{\rm th}$ resonant wave (2.1) and $(\mathbf{X},T)$ are slow variables. The degeneracy in the polarization vector is neglected by the assumption that the incident wave is linearly polarized with the polarization vector $\mathbf{e}_{\rm in} = \mathbf{e}_{\mathbf{k}_{\rm in}}$.

The periodic structure of the photonic crystal is described by the triple Fourier series (2.5) in terms of the reciprocal lattice vectors $\mathbf{k}_1$, $\mathbf{k}_2$, and $\mathbf{k}_3$. For the cubic lattice crystal (2.7), the triple Fourier series for $n_1(\mathbf{x})$ and $n_2(\mathbf{x})$ are simplified as follows:

$$n_1(\mathbf{x}) = n_0 \sum_{(n,m,l)\in\mathbb{Z}^3} \alpha_{n,m,l} e^{ik_0(nx+my+lz)}, \quad n_2(\mathbf{x}) = n_0 \sum_{(n,m,l)\in\mathbb{Z}^3} \beta_{n,m,l} e^{ik_0(nx+my+lz)}, \quad (3.4)$$

where the Fourier coefficients $\alpha_{n,m,l}$ and $\beta_{n,m,l}$ are defined by the material parameters of the cubic crystal. The factor n_0 in (3.4) is taken for convenience. If n_0 is the mean value of $n_0(\mathbf{x})$, then $\alpha_{0,0,0} = 0$. On the other hand, $\beta_{0,0,0}$ is the mean value of the Kerr nonlinearity, which is generally non-zero.

An incident wave with the wave vector $\mathbf{k_{in}}$ generates infinitely many Bloch waves (2.6) due to interaction with the periodic crystal structure. Therefore, the first-order correction term $\mathbf{E}_1(\mathbf{x},t)$ will include infinitely many terms from solutions of the non-homogeneous linear problem:

$$\nabla^2\mathbf{E}_1 - \frac{n_0^2}{c^2}\frac{\partial^2\mathbf{E}_1}{\partial t^2} = 2\frac{n_0^2\omega}{c^2}\frac{\partial^2\mathbf{E}_0}{\partial T\partial t} - 2k\left(\nabla\cdot\nabla_X\right)\mathbf{E}_0$$
$$+\frac{2n_0n_1(\mathbf{x})}{c^2}\frac{\partial^2\mathbf{E}_0}{\partial t^2} + \frac{2n_0n_2(\mathbf{x})}{c^2}|\mathbf{E}_0|^2\frac{\partial^2\mathbf{E}_0}{\partial t^2} + \frac{2}{n_0}\nabla\left(\nabla n_1\cdot\mathbf{E}_0\right) + \frac{2}{n_0}\nabla\left(\nabla\cdot n_2|\mathbf{E}_0|^2\mathbf{E}_0\right), \quad (3.5)$$

where $\nabla_X = (\partial_X, \partial_Y, \partial_Z)$ and the second equation (1.1) has been used. The coupled-mode equations for amplitudes $A_j(\mathbf{X},T)$ are derived from secular terms in the right-hand-side of the nonhomogeneous equation (3.5), which represent solutions of the homogeneous problem. The secular terms lead to the growth of $\mathbf{E}_1(\mathbf{x},t)$ in t, unless they are identically zero. The latter conditions define the coupled-mode equations for amplitudes $A_j(\mathbf{X},T)$, $j = 1,...,N$ in the general form:

$$2ik^2\left(\frac{\partial A_j}{\partial T} + \left(\frac{\mathbf{k}_j}{k}\cdot\nabla_X\right)A_j\right) = f_j(A_1,...,A_N), \qquad j = 1,...,N, \quad (3.6)$$

where the functions $f_j(A_1,...,A_N)$ include the linear and nonlinear terms derived from the triple Fourier series (3.4). The explicit forms of the coupled-mode equations are derived below for two and four counter-propagating resonant Bloch waves, as well as for two oblique resonant waves.

3.1 Coupled-mode equations for two counter-propagating waves

The lowest-order Bragg resonance for two counter-propagating waves (2.16) occurs for $r = 1$, when

$$\mathbf{k}_1 = \frac{\pi}{a}(0,0,1), \qquad \mathbf{k}_2 = \frac{\pi}{a}(0,0,-1). \quad (3.7)$$

Let $A_1 = A_+(Z,T)$ and $A_2 = A_-(Z,T)$ be the amplitudes of the right (forward) and left (backward) propagating waves, respectively. The envelope amplitudes are not modulated across the (X,Y)-plane, since the coupled-mode equations for $A_\pm$ are essentially one-dimensional. The polarization vectors are chosen in the x-direction, such that $\mathbf{e}_{\mathbf{k}_1} = \mathbf{e}_{\mathbf{k}_2} = (1,0,0)$.

The non-homogeneous equations (3.5) can be rewritten for

$$\mathbf{E}_0 = (E_{0,x}(z,t),0,0)\,e^{-i\omega t}, \qquad \mathbf{E}_1 = (E_{1,x}(z,t),0,0)\,e^{-i\omega t}$$

as follows:

$$\frac{\partial^2 E_{1,x}}{\partial z^2} + k^2 E_{1,x} = -2k\frac{\partial^2}{\partial Z \partial z} E_{0,x} - 2ik^2 \frac{\partial}{\partial T} E_{0,x} - \frac{2k^2 n_1(\mathbf{x})}{n_0} E_{0,x} - \frac{2k^2 n_2(\mathbf{x})}{n_0} |E_{0,x}|^2 E_{0,x}. \quad (3.8)$$

Removing the resonant terms at $e^{\pm ikz}$, the coupled-mode equations for amplitudes $A_\pm(Z,T)$ are derived as follows:

$$\begin{aligned} i\left(\frac{\partial A_+}{\partial T} + \frac{\partial A_+}{\partial Z}\right) &+ \alpha_{0,0,1} A_- + \beta_{0,0,0}\left(|A_+|^2 + 2|A_-|^2\right) A_+ \\ &+ \beta_{0,0,1}\left(2|A_+|^2 + |A_-|^2\right) A_- + \beta_{0,0,-1} A_+^2 \bar{A}_- + \beta_{0,0,2} \bar{A}_+ A_-^2 = 0, \quad (3.9) \\ i\left(\frac{\partial A_-}{\partial T} - \frac{\partial A_-}{\partial Z}\right) &+ \alpha_{0,0,-1} A_+ + \beta_{0,0,0}\left(2|A_+|^2 + |A_-|^2\right) A_- \\ &+ \beta_{0,0,-1}\left(|A_+|^2 + 2|A_-|^2\right) A_+ + \beta_{0,0,1} \bar{A}_+ A_-^2 + \beta_{0,0,-2} A_+^2 \bar{A}_- = 0. \quad (3.10) \end{aligned}$$

The coupled-mode equations (3.9)–(3.10) are defined in the domain: $Z \in [0, L_z]$ and $T \geq 0$, where the end points at $Z = 0$ and $Z = L_z$ are the left and right (x, y)-planes, which cut a slice of the photonic crystal. The system is reviewed in [8, 21] for $\beta_{0,0,1} = \beta_{0,0,2} = 0$ and analyzed in [13, 14] for $\beta_{0,0,1} \neq 0$ and $\beta_{0,0,2} = 0$. When $\beta_{0,0,1}, \beta_{0,0,2} \neq 0$, the system (3.9)–(3.10) is the most general coupled-mode system for Bragg resonance of counter-propagating waves [6, 20].

3.2 Coupled-mode equations for four counter-propagating waves

The lowest-order resonance for four counter-propagating waves (2.13) occurs for $p = q = 1$, when

$$\mathbf{k}_1 = \frac{\pi}{a}(1,1,0), \quad \mathbf{k}_2 = \frac{\pi}{a}(1,-1,0), \quad \mathbf{k}_3 = \frac{\pi}{a}(-1,1,0), \quad \mathbf{k}_4 = \frac{\pi}{a}(-1,-1,0). \quad (3.11)$$

Let $A_1 = A_+(X,Y,T)$ and $A_4 = A_-(X,Y,T)$ be the amplitudes of the counter-propagating waves along the main diagonal of the (x,y) plane, while $A_2 = B_+(X,Y,T)$ and $A_3 = B_-(X,Y,T)$ be the amplitudes of the counter-propagating waves along the anti-diagonal of the (x,y)-plane. The envelope amplitudes are not modulated in the Z-direction, since the coupled-mode equations for $A_\pm$ and $B_\pm$ are essentially two-dimensional. The polarization vectors are chosen in the z-direction, such that $\mathbf{e}_{\mathbf{k}_j} = (0,0,1)$, $1 \leq j \leq 4$, which corresponds to the TE mode of the photonic crystal.

The non-homogeneous equations (3.5) can be rewritten for

$$\mathbf{E}_0 = (0, 0, E_{0,z}(x,y,t))\, e^{-i\omega t}, \qquad \mathbf{E}_1 = (0, 0, E_{1,z}(x,y,t))\, e^{-i\omega t}$$

as follows:

$$\begin{aligned} \nabla^2 E_{1,z} + k^2 E_{1,z} &= -2k\frac{\partial^2}{\partial X \partial x} E_{0,z} - 2k\frac{\partial^2}{\partial Y \partial y} E_{0,z} - 2ik^2 \frac{\partial}{\partial T} E_{0,z} \\ &- \frac{2k^2 n_1(\mathbf{x})}{n_0} E_{0,z} - \frac{2k^2 n_2(\mathbf{x})}{n_0} |E_{0,z}|^2 E_{0,z}. \quad (3.12) \end{aligned}$$

Removing the resonant terms at $e^{\frac{i}{\sqrt{2}}(\pm kx \pm ky)}$, the coupled-mode equations for amplitudes $A_\pm(X,Y,T)$ and $B_\pm(X,Y,T)$ are derived as follows:

$$i\left(\frac{\partial A_+}{\partial T} + \frac{\partial A_+}{\partial X} + \frac{\partial A_+}{\partial Y}\right) + \alpha_{1,1,0} A_- + \alpha_{0,1,0} B_+ + \alpha_{1,0,0} B_- + F_+(A_\pm, B_\pm) = 0, \quad (3.13)$$

$$i\left(\frac{\partial A_-}{\partial T} - \frac{\partial A_-}{\partial X} - \frac{\partial A_-}{\partial Y}\right) + \alpha_{-1,-1,0}A_+ + \alpha_{-1,0,0}B_+ + \alpha_{0,-1,0}B_- + F_-(A_\pm, B_\pm) = 0, \quad (3.14)$$

$$i\left(\frac{\partial B_+}{\partial T} + \frac{\partial B_+}{\partial X} - \frac{\partial B_+}{\partial Y}\right) + \alpha_{0,-1,0}A_+ + \alpha_{1,0,0}A_- + \alpha_{1,-1,0}B_- + G_+(A_\pm, B_\pm) = 0, \quad (3.15)$$

$$i\left(\frac{\partial B_-}{\partial T} - \frac{\partial B_-}{\partial X} + \frac{\partial B_-}{\partial Y}\right) + \alpha_{-1,0,0}A_+ + \alpha_{0,1,0}A_- + \alpha_{-1,1,0}B_+ + G_-(A_\pm, B_\pm) = 0, \quad (3.16)$$

where $F_\pm$ and $G_\pm$ are cubic nonlinear functions, which are given explicitly in Appendix A. The coupled-mode equations (3.13)–(3.16) are defined in the domain: $(X, Y) \in \mathcal{D}$ and $T \geq 0$, where $\mathcal{D}$ is the (x, y)-plane of the photonic crystal, which is cut at the rectangle with sides of length L_ξ and L_η, rotated on 45° in characteristic coordinates (ξ, η). The system has not been previously studied in literature, to the best of our knowledge. The linear part of the system (3.13)–(3.16) will be analyzed in the next section.

3.3 Coupled-mode equations for two oblique waves

Two oblique resonant waves on the (x, y)-plane are defined by the resonant wave vectors (2.15) under the constraint (2.16). Assuming that $\mathbf{e}_1 = \mathbf{e}_2 = (0, 0, 1)$, the Maxwell equations can be reduced to the same form (3.12), where the resonant terms are eliminated at the wave vectors $\mathbf{k}_1$ and $\mathbf{k}_2$. The coupled-mode equations for amplitudes $A_{1,2}(X, Y, T)$ are derived as follows:

$$i\left(\frac{\partial A_1}{\partial T} + \frac{p}{\sqrt{p^2+q^2}}\frac{\partial A_1}{\partial X} + \frac{q}{\sqrt{p^2+q^2}}\frac{\partial A_1}{\partial Y}\right) + \alpha_{-n,-m,0}A_2 + \beta_{0,0,0}\left(|A_1|^2 + 2|A_2|^2\right)A_1$$
$$+\beta_{-n,-m,0}\left(2|A_1|^2 + |A_2|^2\right)A_2 + \beta_{n,m,0}A_1^2\bar{A}_2 + \beta_{-2n,-2m,0}\bar{A}_1A_2^2 = 0, \quad (3.17)$$

$$i\left(\frac{\partial A_2}{\partial T} + \frac{p+2n}{\sqrt{p^2+q^2}}\frac{\partial A_2}{\partial X} + \frac{q+2m}{\sqrt{p^2+q^2}}\frac{\partial A_2}{\partial Y}\right) + \alpha_{n,m,0}A_1 + \beta_{0,0,0}\left(2|A_1|^2 + |A_2|^2\right)A_1$$
$$+\beta_{n,m,0}\left(|A_1|^2 + 2|A_2|^2\right)A_1 + \beta_{-n,-m,0}\bar{A}_1A_2^2 + \beta_{2n,2m,0}A_1^2\bar{A}_2 = 0. \quad (3.18)$$

Coupled-mode equations (3.17)–(3.18) for two oblique waves can not be reduced to the one-dimensional system (3.9)–(3.10), since the characteristics in the system (3.17)–(3.18) are no longer parallel.

The coupled-mode equations for three oblique resonant waves (2.17) can be derived similarly, subject to the resonance condition (2.18). Three characteristics along the wave vectors $\mathbf{k}_{1,2,3}$ belong to the same (X, Y)-plane and therefore, the stationary transmission problem is a boundary-value problem on the (X, Y)-plane with the three linearly dependent, characteristic coordinates. Oblique interaction of resonant Bloch waves was recently addressed in [17], where numerical solutions were constructed for three oblique waves in a hexagonal crystal.

4 Analysis of stationary transmission

The stationary transmission problem follows from the separation of variables in the coupled-mode equations (3.6):

$$A_j(\mathbf{X}, T) = a_j(\mathbf{X})e^{-i\Omega T}, \qquad j = 1, ..., N, \quad (4.1)$$

where Ω is the detuning frequency. When the boundary-value problem for $a_j(\mathbf{X})$ is well-posed in a bounded domain, analytical solutions for the linear stationary coupled-mode equations can be derived by using the separation of variables and generalized Fourier series [22]. Exploiting these analytical solutions, integral invariants of the stationary transmission, reflection and diffraction of the resonant Bloch waves can be computed explicitly.

For further consideration, we simplify the geometric configuration of the photonic crystal, by assuming that the crystal is isotropic in all directions and symmetric with respect to the origin $(0,0,0)$, the latter property can be achieved by a simple shift of (x,y,z). Coefficients $\alpha_{n,m,l}$ of the Fourier series (3.4) satisfy the constraints:

$$\alpha_{n,m,l} = \bar{\alpha}_{-n,-m,-l}, \tag{4.2}$$

due to the reality of $n_1(\mathbf{x})$,

$$\alpha_{n,m,l} = \alpha_{m,n,l} = \alpha_{n,l,m} = \alpha_{l,m,n}, \tag{4.3}$$

due to the crystal isotropy, and

$$\alpha_{-n,m,l} = \alpha_{n,m,l}, \quad \alpha_{n,-m,l} = \alpha_{n,m,l}, \quad \alpha_{n,m,-l} = \alpha_{n,m,l}, \tag{4.4}$$

due to the crystal symmetry. Linear stationary coupled-mode equations are analyzed below for two and four counter-propagating resonant Bloch waves, as well as for two oblique resonant waves.

4.1 Transmission of two counter-propagating waves

After the separation of variables (4.1) and the linearization of the coupled-mode equations (3.9)–(3.10), the amplitudes $a_\pm(Z)$ satisfy the system of ordinary differential equations:

$$i\frac{da_+}{dZ} + \Omega a_+ + \alpha a_- = 0, \tag{4.5}$$

$$-i\frac{da_-}{dZ} + \alpha a_+ + \Omega a_- = 0, \tag{4.6}$$

where

$$\alpha = \alpha_{0,0,1} = \alpha_{0,0,-1} \in \mathbb{R}, \tag{4.7}$$

due to the constraints (4.2) and (4.4). The problem (4.5)–(4.6) is defined on the finite interval $0 \le Z \le L_Z$. When the incident wave is illuminated to the photonic crystal from the left, the linear system (4.5)–(4.6) is completed by the boundary conditions:

$$a_+(0) = \alpha_+, \qquad a_-(L_Z) = 0, \tag{4.8}$$

where α_+ is the given amplitude of the incident wave at the left (x,y)-plane of the crystal. The general solution of the ODE system (4.5)–(4.6) is given explicitly as follows:

$$\begin{pmatrix} a_+ \\ a_- \end{pmatrix} = c_+ \begin{pmatrix} \alpha \\ \Omega + i\kappa \end{pmatrix} e^{\kappa Z} + c_- \begin{pmatrix} \alpha \\ \Omega - i\kappa \end{pmatrix} e^{-\kappa Z}, \tag{4.9}$$

where $c_\pm \in \mathbb{C}$ are arbitrary and $\kappa \in \mathbb{C}$ is the root of the determinant equation:

$$\kappa = \sqrt{\alpha^2 - \Omega^2}. \tag{4.10}$$

When $\kappa = iK$, $K \in \mathbb{R}$, the linear dispersion relation $\Omega = \Omega(K)$ follows from the quadratic equation:

$$\Omega^2 = \alpha^2 + K^2. \tag{4.11}$$

The two branches of (4.11) correspond to the two counter-propagating resonant waves. Their resonance leads to the photonic band gap, which is located in the interval: $|\Omega| < |\alpha|$. Let $\Omega = 0$ for simplicity, i.e. the detuning frequency is fixed in the middle of the band gap. The unique solution of the boundary-value problem (4.8) follows from the general solution (4.9):

$$\begin{pmatrix} a_+ \\ a_- \end{pmatrix} = \frac{\alpha_+}{\cosh \alpha L_Z} \begin{pmatrix} \cosh \alpha (L_Z - Z) \\ -i \sinh \alpha (L_Z - Z) \end{pmatrix}. \tag{4.12}$$

The transmittance T and reflectance R are defined from the other boundary values of the solution (4.12):

$$T = \left| \frac{a_+(L_Z)}{a_+(0)} \right|^2 = \frac{1}{\cosh^2 \alpha L_Z}, \qquad R = \left| \frac{a_-(0)}{a_+(0)} \right|^2 = \frac{\sinh^2 \alpha L_Z}{\cosh^2 \alpha L_Z}, \tag{4.13}$$

such that the balance identity $T + R = 1$ is satisfied. The analytical solution (4.12) for the two counter-propagating waves is well-known [21] and is reproduced here for comparison with the case of four counter-propagating and two oblique waves on the plane.

4.2 Transmission of four counter-propagating waves

The stationary transmission of four counter-propagating waves in the coupled-mode equations (3.13)–(3.16) is studied in the characteristic coordinates (ξ, η):

$$\xi = \frac{X + Y}{2}, \qquad \eta = \frac{X - Y}{2}. \tag{4.14}$$

After the separation of variables (4.1) and the linearization of the coupled-mode equations (3.13)–(3.16), the amplitudes $a_\pm(\xi, \eta)$ and $b_\pm(\xi, \eta)$ satisfy the system of partial differential equations:

$$\begin{aligned}
i\frac{\partial a_+}{\partial \xi} + \Omega a_+ + \alpha a_- + \beta b_+ + \beta b_- &= 0, && (4.15)\\
-i\frac{\partial a_-}{\partial \xi} + \alpha a_+ + \Omega a_- + \bar{\beta} b_+ + \bar{\beta} b_- &= 0, && (4.16)\\
i\frac{\partial b_+}{\partial \eta} + \bar{\beta} a_+ + \beta a_- + \Omega b_+ + \alpha b_- &= 0, && (4.17)\\
-i\frac{\partial b_-}{\partial \eta} + \bar{\beta} a_+ + \beta a_- + \alpha b_+ + \Omega b_- &= 0, && (4.18)
\end{aligned}$$

where

$$\alpha = \alpha_{1,1,0} = \alpha_{-1,-1,0} = \alpha_{1,-1,0} = \alpha_{-1,1,0} \in \mathbb{R} \tag{4.19}$$

and

$$\beta = \alpha_{0,1,0} = \alpha_{1,0,0} = \bar{\alpha}_{0,-1,0} = \bar{\alpha}_{-1,0,0} \in \mathbb{C}, \tag{4.20}$$

due to the constraints (4.2)–(4.4). The problem (4.15)–(4.18) is defined in a bounded domain on the plane (ξ, η). We consider the rectangle,

$$\mathcal{D} = \{(\xi, \eta) : \ 0 \leq \xi \leq L_\xi, \ 0 \leq \eta \leq L_\eta\}, \tag{4.21}$$

which corresponds to a rectangle in physical coordinates (X, Y), rotated at 45° in characteristic coordinates (ξ, η). When the incident wave is illuminated from the left along the main diagonal in the (X, Y)-plane of the photonic crystal, the linear system (4.15)–(4.18) is completed by the boundary conditions:

$$a_+(0, \eta) = \alpha_+(\eta), \qquad a_-(L_\xi, \eta) = 0, \qquad b_+(\xi, 0) = 0, \qquad b_-(\xi, L_\eta) = 0, \tag{4.22}$$

where $\alpha_+(\eta)$ is the given amplitude of the incident wave at the left boundary of the crystal. The linear dispersion relation $\Omega = \Omega(K_\xi, K_\eta)$, where (K_ξ, K_η) are Fourier wave numbers, follows from the determinant equation of the linear PDE system (4.15)–(4.18).

Lemma 4.1 *The linear dispersion relation $\Omega = \Omega(K_\xi, K_\eta)$ is defined by roots of $D(\Omega, K_\xi, K_\eta)$, where*

$$D(\Omega, K_\xi, K_\eta) = (\Omega^2 - \alpha^2 - K_\xi^2)(\Omega^2 - \alpha^2 - K_\eta^2) - 4|\beta|^2\Omega^2 + 2\alpha(\beta + \bar{\beta})^2\Omega - 2\alpha^2(\beta^2 + \bar{\beta}^2). \tag{4.23}$$

Proof. The determinant equation follows from the PDE system (4.15)–(4.18) for the Fourier modes $e^{i(K_\xi \xi + K_\eta \eta)}$ in the explicit form:

$$D(\Omega, K_\xi, K_\eta) = \begin{vmatrix} \Omega - K_\xi & \alpha & \beta & \beta \\ \alpha & \Omega + K_\xi & \bar{\beta} & \bar{\beta} \\ \bar{\beta} & \beta & \Omega - K_\eta & \alpha \\ \bar{\beta} & \beta & \alpha & \Omega + K_\eta \end{vmatrix}. \tag{4.24}$$

Although the straightforward computations of $D(\Omega, K_\xi, K_\eta)$ are involved technically, it is easy to compute the partial derivatives of $D(\Omega, K_\xi, K_\eta)$:

$$\frac{\partial D}{\partial K_\xi} = -2K_\xi \left(\Omega^2 - \alpha^2 - K_\eta^2\right), \tag{4.25}$$

$$\frac{\partial D}{\partial K_\eta} = -2K_\eta \left(\Omega^2 - \alpha^2 - K_\xi^2\right), \tag{4.26}$$

$$\frac{\partial D}{\partial \Omega} = 2\Omega \left(\Omega^2 - \alpha^2 - K_\xi^2\right) + 2\Omega \left(\Omega^2 - \alpha^2 - K_\eta^2\right) - 8|\beta|^2\Omega + 2\alpha(\beta + \bar{\beta})^2. \tag{4.27}$$

In addition, the value $D(0, 0, 0)$ follows from (4.24):

$$D(0, 0, 0) = \alpha^4 - 2\alpha^2(\beta^2 + \bar{\beta}^2). \tag{4.28}$$

Integrating (4.25)–(4.27) with the particular value (4.28), we find that $D(\Omega, K_\xi, K_\eta)$ is given by (4.23). ∎

Four surfaces of the dispersion relations are defined on (K_ξ, K_η) by roots of the determinant equation (4.23). These surfaces correspond to the four resonant Bloch waves. Two surfaces for $\Omega > 0$ are shown on Fig. 1 for $\alpha = 1$ and $\beta = i$. It follows from the figure that there exists a stop band between four resonant counter-propagating waves, which is located for $|\Omega| < |\alpha|$, when $\beta \in i\mathbb{R}$.

Let $\Omega = 0$ for simplicity, i.e. the detuning frequency is fixed in the middle of the stop bands between each pair of the counter-propagating waves. The unique Fourier series solutions of the boundary-value problem (4.22) can be found with the method of separation of variables [22], which reduces the PDE problem to two ODE problems. Using the particular form (4.15)–(4.18), the separation of variables is given by the ansatz:

$$a_+(\xi,\eta) = u_+(\xi) w_a(\eta), \qquad a_-(\xi,\eta) = u_-(\xi) w_a(\eta) \tag{4.29}$$

$$b_+(\xi,\eta) = w_b(\xi) v_+(\eta), \qquad b_-(\xi,\eta) = w_b(\xi) v_-(\eta), \tag{4.30}$$

where

$$v_+(\eta) + v_-(\eta) = \mu w_a(\eta), \qquad \bar{\beta} u_+(\xi) + \beta u_-(\xi) = -\lambda w_b(\xi), \tag{4.31}$$

constants (λ, μ) are arbitrary parameters, and vectors $(u_+, u_-)^T$ and $(v_+, v_-)^T$ solve the two uncoupled ODE systems:

$$\begin{pmatrix} i\partial_\xi & \alpha \\ \alpha & -i\partial_\xi \end{pmatrix} \begin{pmatrix} u_+ \\ u_- \end{pmatrix} = \Gamma^{-1} \begin{pmatrix} |\beta|^2 & \beta^2 \\ \bar{\beta}^2 & |\beta|^2 \end{pmatrix} \begin{pmatrix} u_+ \\ u_- \end{pmatrix} \tag{4.32}$$

and

$$\begin{pmatrix} i\partial_\eta & \alpha \\ \alpha & -i\partial_\eta \end{pmatrix} \begin{pmatrix} v_+ \\ v_- \end{pmatrix} = \Gamma \begin{pmatrix} 1 & 1 \\ 1 & 1 \end{pmatrix} \begin{pmatrix} v_+ \\ v_- \end{pmatrix}, \tag{4.33}$$

where $\Gamma = \lambda/\mu$. The boundary conditions for (4.32)–(4.33) follows from (4.22) as follows:

$$u_+(0) = 1, \qquad u_-(L_\xi) = 0, \tag{4.34}$$

and

$$v_+(0) = v_-(L_\eta) = 0. \tag{4.35}$$

The homogeneous problem (4.33) and (4.35) defines the spectrum of Γ, while the inhomogeneous problem (4.32) and (4.34) defines a unique particular solution (4.29)–(4.30). The general solution of the problem (4.15)–(4.18) with the boundary values (4.22) is thought to be a linear superposition of infinitely many particular solutions, if the convergence and completeness of the decomposition formulas can be proved [22]. We first give solutions of the two problems above and then consider the orthogonality and completeness of the generalized Fourier series.

Lemma 4.2 *All eigenvalues Γ of the homogeneous problem (4.33) and (4.35) are given by non-zero roots of the characteristic equation:*

$$\mathcal{R} = \left\{ k \in \mathbb{C} : \left(\frac{k-\alpha}{k+\alpha} \right)^2 e^{-2ikL_\eta} = 1, \ \mathrm{Re}(k) \geq 0, \ k \neq 0 \right\}, \tag{4.36}$$

such that

$$\Gamma = \frac{\alpha^2 + k^2}{2\alpha}. \tag{4.37}$$

Proof. The general solution of the ODE system (4.33) with the use of (4.37) is found explicitly as follows:

$$\begin{pmatrix} v_+ \\ v_- \end{pmatrix} = c_k \begin{pmatrix} \alpha - k \\ \alpha + k \end{pmatrix} e^{ik\eta} + c_{-k} \begin{pmatrix} \alpha + k \\ \alpha - k \end{pmatrix} e^{-ik\eta}. \tag{4.38}$$

The coefficients c_k and c_{-k} satisfy the relations due to the boundary conditions (4.35):

$$\frac{c_k}{c_{-k}} = \frac{k+\alpha}{k-\alpha} = \frac{k-\alpha}{k+\alpha} e^{-2ikL_\eta}, \tag{4.39}$$

from which the characteristic equation (4.36) for roots $k \in \mathbb{C}$ follows. The roots k and $(-k)$ correspond to the same Γ and $v_\pm(\eta)$. The root $k = 0$ corresponds to the zero solution for $v_\pm(\eta)$. Therefore, the roots $k = 0$ and $\mathrm{Re}(k) < 0$ are excluded from $\mathcal{R}$. ∎

Roots $k \in \mathcal{R}$ and $(-k) \in \mathcal{R}$ are shown on Figure 2 from the numerical solution of the characteristic equation (4.36) for $\alpha = 1$ and $L_\eta = 10$. It follows from the figure that all roots $k \in \mathcal{R}$ are isolated points, which accumulate to the real axis of k at infinity. The standard analysis of analytical functions at infinity leads to the asymptotic formula for distribution of large roots k in the domain $|k| > k_0 \gg 1$:

$$k_{+j} = \frac{2\pi j}{L_\eta} + \frac{i\alpha}{\pi j} + \mathrm{O}\left(\frac{1}{j^2}\right), \qquad k_{-j} = \frac{\pi(1+2j)}{L_\eta} + \frac{2i\alpha}{\pi(1+2j)} + \mathrm{O}\left(\frac{1}{j^2}\right), \tag{4.40}$$

where $j \in \mathbb{Z}_+$. The leading order of the asymptotic approximation (4.40) is also shown on Fig. 2 by dotted curves. It follows from (4.36) that there exist two sets of roots $\mathcal{R}_+$ and $\mathcal{R}_-$, such that $\mathcal{R}_+ \cup \mathcal{R}_- = \mathcal{R}$, where

$$\mathcal{R}_\pm = \left\{ k \in \mathbb{C} : \ \frac{k-\alpha}{k+\alpha} e^{-ikL_\eta} = \pm 1, \ \mathrm{Re}(k) \geq 0, \ k \neq 0 \right\}. \tag{4.41}$$

The eigenfunction $v(\eta) = v_+(\eta) + v_-(\eta)$ is symmetric (anti-symmetric) with respect to $\eta = L_\eta/2$ for $k \in \mathcal{R}_+$ ($k \in \mathcal{R}_-$). Moreover, explicit formulas for $v(\eta)$ follow from (4.38) and (4.39):

$$k \in \mathcal{R}_+ : \ v(\eta) = c_+ \cos k\left(\frac{L_\eta}{2} - \eta\right), \tag{4.42}$$

$$k \in \mathcal{R}_- : \ v(\eta) = c_- \sin k\left(\frac{L_\eta}{2} - \eta\right), \tag{4.43}$$

where (c_+, c_-) are normalization constants. Asymptotic solutions (4.40) correspond to two sets of eigenfunctions

$$\left\{ \cos(\pi j \eta'), \ \ \sin\left(\frac{\pi(2j+2)\eta'}{2}\right) \right\}_j, \qquad \eta' = \frac{2\eta}{L_\eta} - 1, \tag{4.44}$$

which solve the homogeneous Neumann's problem on the normalized interval $-1 \leq \eta' \leq 1$.

Lemma 4.3 *Let Γ be an eigenvalue (4.37) for some $k \in \mathcal{R}$. Assume that the following constraint is satisfied:*

$$u_0 = \lambda_k(\alpha^2 + k^2)\cos\alpha\lambda_k L_\xi + 2i|\beta|^2 \sin\alpha\lambda_k L_\xi \neq 0, \tag{4.45}$$

where

$$\lambda_k = \sqrt{\frac{2(\beta^2 + \bar{\beta}^2)}{\alpha^2 + k^2} - 1}. \tag{4.46}$$

Then, there exists a unique solution of the non-homogeneous problem (4.32) and (4.34) for this Γ.

Proof. A general solution of the ODE system (4.32) is found explicitly as follows:

$$\begin{pmatrix} u_+ \\ u_- \end{pmatrix} = d_k \begin{pmatrix} \alpha^2 + k^2 - 2\beta^2 \\ \lambda_k(\alpha^2 + k^2) + 2|\beta|^2 \end{pmatrix} e^{i\alpha\lambda_k\eta} + d_{-k} \begin{pmatrix} \alpha^2 + k^2 - 2\beta^2 \\ -\lambda_k(\alpha^2 + k^2) + 2|\beta|^2 \end{pmatrix} e^{-i\alpha\lambda_k\eta}, \tag{4.47}$$

As one can expect, it follows from the determinant equation (4.23) that $D(0, \alpha\lambda_k, k) = 0$. Using the boundary conditions (4.34), coefficients d_k and d_{-k} are found uniquely, under the constraint (4.45). ∎

If $u_0 \neq 0$, solutions of the non-homogeneous problem (4.32) and (4.34) with the normalization $u_+(0) = u_0$ are written in the explicit form:

$$\begin{pmatrix} u_+ \\ u_- \end{pmatrix} = \lambda_k(\alpha^2 + k^2) \begin{pmatrix} 1 \\ 0 \end{pmatrix} \cos\alpha\lambda_k(L_\xi - \xi) + i \begin{pmatrix} 2|\beta|^2 \\ \alpha^2 + k^2 - 2\bar{\beta}^2 \end{pmatrix} \sin\alpha\lambda_k(L_\xi - \xi). \tag{4.48}$$

If $u_0 = 0$ for some Γ, there exist a solution of the homogeneous version of the problem (4.32) and (4.34) for the same eigenvalue Γ^{-1}. Therefore, if $u_0 = 0$ for some Γ, the system of coupled equations (4.15)–(4.18) for $\Omega = 0$ has a non-trivial waveguide mode, which satisfies the boundary conditions (4.22) with $\alpha_+ = 0$. When the incident light is illuminated with $\alpha_+ \neq 0$, the waveguide mode grows secularly in time t, such that no bounded solution of the stationary problem (4.15)–(4.18) and (4.22) with $\alpha_+ \neq 0$ exists. In what follows, we assume that $u_0 \neq 0$ for all $k \in \mathcal{R}$.

According to the representation (4.29) for $\alpha_+(\eta) = a_+(0, \eta)$, we need completeness and convergence of series of scalar eigenfunctions $v(\eta) = v_+(\eta) + v_-(\eta)$, defined for roots $k \in \mathcal{R}$. The scalar decomposition of $\alpha_+(\eta)$ in series of eigenfunctions $v(\eta)$ follows from results on orthogonality and completeness of the eigenfunctions $v(\eta)$.

Lemma 4.4 *Assume that all roots $k \in \mathcal{R}$ are simple and non-degenerate, such that*

$$(k^2 - \alpha^2)L_\eta + 2i\alpha \neq 0. \tag{4.49}$$

Then, there exists a set of normalized eigenfunctions $v_j(\eta)$ for distinct roots $k = k_j \in \mathcal{R}$, which are orthogonal as follows:

$$\int_0^{L_\eta} v_i(\eta) v_j(\eta) d\eta = \delta_{i,j}. \tag{4.50}$$

Proof. The set of adjoint eigenvectors to the problem (4.33) and (4.35) with respect to the standard inner product in $L^2([0, L_\eta])$ is given by the vectors $(\bar{v}_-, \bar{v}_+)^T$. As a result, the scalar eigenfunctions $v_j(\eta)$ for distinct roots $k = k_j$ satisfy the orthogonality relations (4.50) with $i \neq j$. The scalar eigenfunction $v(\eta)$ is found from (4.38) and (4.39) in the explicit form:

$$v(\eta) = c_0 \left(k \cos k\eta + i\alpha \sin k\eta \right), \tag{4.51}$$

where c_0 is a normalization constant. Integrating $v^2(\eta)$ on $\eta \in [0, L_\eta]$, we confirm that the eigenfunctions $v_j(\eta)$ can be normalized by the inner product (4.50) with $i = j$, if the constraint (4.49) is met. ∎

Proposition 4.5 *Assume that the constraint (4.49) is satisfied for any $k \in \mathcal{R}$. Then, any continuously differentiable complex-valued function $f(\eta)$ on $0 \leq \eta \leq L_\eta$ is uniquely represented by the series of eigenfunctions:*

$$f(\eta) = \sum_{\text{all } k_j \in \mathcal{R}} c_j v_j(\eta), \qquad c_j = \int_0^{L_\eta} f(\eta) v_j(\eta) d\eta, \tag{4.52}$$

and the series converges to $f(\eta)$ uniformly on $0 \leq \eta \leq L_\eta$.

Proof. It follows from (4.33) and (4.35) that the scalar eigenfunction $v(\eta)$ solves the second-order boundary-value problem:

$$v'' + k^2 v = 0, \tag{4.53}$$

such that

$$iv'(0) + \alpha v(0) = 0, \qquad -iv'(L_\eta) + \alpha v(L_\eta) = 0. \tag{4.54}$$

The Sommerfeld radiation boundary conditions (4.54) explain why the spectrum of the formally self-adjoint operator (4.53) is complex-valued. The statement of Proposition follows from Expansion Theorem [7, p.303], since the theorem's condition is satisfied: $A_{2,4} = 1$, where $A_{2,4}$ is the determinant of the second and fourth columns of the matrix A, associated with the boundary conditions:

$$A = \begin{pmatrix} \alpha & i & 0 & 0 \\ 0 & 0 & \alpha & -i \end{pmatrix}.$$

As a result, the Fourier cosine-series of eigenfunctions (4.44) approximates the series expansion (4.52) for large roots $k = k_{\pm j}$ uniformly on $\eta \in [0, L_\eta]$. The uniform convergence of (4.52) follows from that of the Fourier cosine-series [22]. ∎

Using the method of separation of variables and convergence of series of eigenfunctions, we summarize the existence and uniqueness results on the generalized Fourier series solutions of the linear boundary-value problem (4.15)–(4.18) and (4.22) with $\Omega = 0$.

Proposition 4.6 *Assume that the constraints (4.45) and (4.49) are satisfied for all roots $k \in \mathcal{R}$. Let the set $\{c_j\}$ be uniquely defined by the series (4.52) for $f(\eta) = \alpha_+(\eta)$. Then, there exists*

a unique continuously differentiable solution of the boundary-value problem (4.15)–(4.18) and (4.22) with $\Omega = 0$ in the domain (4.21):

$$a_+(\xi,\eta) = \sum_{\text{all } k_j \in \mathcal{R}} c_j \frac{u_{+j}(\xi)}{u_{+j}(0)} \left(v_{+j}(\eta) + v_{-j}(\eta)\right), \tag{4.55}$$

$$a_-(\xi,\eta) = \sum_{\text{all } k_j \in \mathcal{R}} c_j \frac{u_{-j}(\xi)}{u_{+j}(0)} \left(v_{+j}(\eta) + v_{-j}(\eta)\right), \tag{4.56}$$

$$b_+(\xi,\eta) = -\sum_{\text{all } k_j \in \mathcal{R}} c_j \frac{\bar{\beta} u_{+j}(\xi) + \beta u_{-j}(\xi)}{\Gamma_j u_{+j}(0)} v_{+j}(\eta), \tag{4.57}$$

$$b_-(\xi,\eta) = -\sum_{\text{all } k_j \in \mathcal{R}} c_j \frac{\bar{\beta} u_{+j}(\xi) + \beta u_{-j}(\xi)}{\Gamma_j u_{+j}(0)} v_{-j}(\eta). \tag{4.58}$$

We illustrate the generalized Fourier series solutions (4.55)–(4.58) with two examples: (i) a single term of the generalized Fourier series and (ii) a constant input function $\alpha_+(\eta) = \alpha_+$. For both examples, we compute the integral invariants for the incident ($\mathcal{I}_{\text{in}}$), transmitted ($\mathcal{I}_{\text{out}}$), reflected ($\mathcal{I}_{\text{ref}}$) and diffracted ($\mathcal{I}_{\text{dif}}$) waves from their definitions:

$$\mathcal{I}_{\text{in}} = \int_0^{L_\eta} |a_+(0,\eta)|^2 d\eta, \qquad \mathcal{I}_{\text{out}} = \int_0^{L_\eta} |a_+(L_\xi,\eta)|^2 d\eta, \tag{4.59}$$

$$\mathcal{I}_{\text{ref}} = \int_0^{L_\eta} |a_-(0,\eta)|^2 d\eta, \qquad \mathcal{I}_{\text{dif}} = \int_0^{L_\xi} \left(|b_+(\xi,L_\eta)|^2 + |b_-(\xi,0)|^2\right) d\xi. \tag{4.60}$$

Let the transmittance T, reflectance R and diffractance D be defined from the relations:

$$T = \frac{\mathcal{I}_{\text{out}}}{\mathcal{I}_{\text{in}}}, \qquad R = \frac{\mathcal{I}_{\text{ref}}}{\mathcal{I}_{\text{in}}}, \qquad D = \frac{\mathcal{I}_{\text{dif}}}{\mathcal{I}_{\text{in}}}. \tag{4.61}$$

The integral invariants satisfy the balance identity:

$$R + T + D = 1, \tag{4.62}$$

which follows from integration of the balance equation:

$$\frac{\partial}{\partial \xi}\left(|a_+|^2 - |a_-|^2\right) + \frac{\partial}{\partial \eta}\left(|b_+|^2 - |b_-|^2\right) = 0. \tag{4.63}$$

First, we consider a single term of the Fourier series solutions (4.55)–(4.58) for a root $k \in \mathcal{R}$. The transmittance and reflectance are found from (4.48) in the explicit form:

$$T = \left| \frac{\lambda_k(\alpha^2 + k^2)}{\lambda_k(\alpha^2 + k^2)\cos \alpha\lambda_k L_\xi + 2i|\beta|^2 \sin \alpha\lambda_k L_\xi} \right|^2, \tag{4.64}$$

$$R = \left| \frac{(\alpha^2 + k^2 - 2\bar{\beta}^2)\sin \alpha\lambda_k L_\xi}{\lambda_k(\alpha^2 + k^2)\cos \alpha\lambda_k L_\xi + 2i|\beta|^2 \sin \alpha\lambda_k L_\xi} \right|^2, \tag{4.65}$$

while the diffractance is found from the balance identity as $D = 1 - T - R$. These integral invariants of the stationary transmission are shown on Figure 3(a-c) versus $\text{Re}(k)$, $k \in \mathcal{R}$ for

$\alpha = 1$, $\beta = i$, and $L_\xi = L_\eta = 10$. It is clear from figures that the diffraction is not small for smaller values of $|k|$, but it becomes negligible for larger values of $|k|$. Transmission remains small for all modes, since the detuning frequency is set in the middle of the stop band and the nonlinearities are dropped from the coupled-mode equations (4.15)–(4.18).

Next, we consider a constant input function:

$$\alpha_+(\eta) = \alpha_+, \qquad \eta \in [0, L_\eta], \tag{4.66}$$

when c_j can be found explicitly as:

$$c_j = \frac{4i\alpha\alpha_+}{k[L(k^2 - \alpha^2) + 2i\alpha]}, \qquad k \in \mathcal{R}_+, \tag{4.67}$$

and $c_j = 0$ for $k \in \mathcal{R}_-$. Figures 4(a-d) show the solution surfaces for $|a_\pm(\xi, \eta)|^2$ and $|b_\pm(\xi, \eta)|^2$ in the domain (4.21) for $\alpha = 1$, $\beta = i$, $L_\xi = L_\eta = 10$, and $\alpha_+ = 1$. It is seen from the figures that the boundary conditions (4.22) are satisfied by the truncated generalized Fourier series (4.55)–(4.58) with only 30 first terms.

The Parseval's identity can not be applied to eigenfunctions $v_j(\eta)$, because the inner product (4.50) is not the standard inner product in $L^2([0, L_\eta])$. As a result, the energy spectrum of $I_{\rm out}$, $I_{\rm ref}$, and $I_{\rm dif}$ can not be decomposed into a superposition of the squared amplitudes $|c_j|^2$. Nevertheless, the numerical values for T, R, and D can be found from numerical integration of the solution surfaces (4.59)–(4.60) as follows:

$$T \approx 2.45 \times 10^{-12}, \qquad R \approx 0.9297, \qquad D \approx 0.0703,$$

such that $T + R + D \approx 1$. These values show that the incident wave is reflected from the stop band with energy loss in 7%, which is due to scattering into two transverse diffracted waves.

4.3 Transmission of two oblique waves

The stationary boundary-value problem for the system (3.17)–(3.18) is studied in the characteristic coordinates (ξ, η):

$$\xi = \frac{\sqrt{p^2 + q^2}}{2(pm - nq)} \left((q + 2m)x - (p + 2n)y \right), \tag{4.68}$$

$$\eta = \frac{\sqrt{p^2 + q^2}}{2(pm - nq)} \left(-qx + py \right), \tag{4.69}$$

where the line $\xi = \xi_0$ is orthogonal to $\mathbf{k}_1$ and the line $\eta = \eta_0$ is orthogonal to $\mathbf{k}_2$. After the separation of variables (4.1) and the linearization of the coupled-mode equations (3.17)–(3.18), the amplitudes $a_{1,2}(\xi, \eta)$ satisfy the system of partial differential equations:

$$i\frac{\partial a_1}{\partial \xi} + \Omega a_1 + \alpha a_2 = 0, \tag{4.70}$$

$$i\frac{\partial a_2}{\partial \eta} + \alpha a_1 + \Omega a_2 = 0, \tag{4.71}$$

where

$$\alpha = \alpha_{n,m,0} = \alpha_{-n,-m,0} \in \mathbb{R}, \tag{4.72}$$

due to the constraints (4.2) and (4.4). The problem (4.70)–(4.71) is defined in a bounded domain on the plane (ξ, η), e.g. in the rectangle $\mathcal{D}$, which is given by (4.21). When the incident wave is illuminated in the wave $\mathbf{k}_1$ but not in the wave $\mathbf{k}_2$, the linear system (4.70)–(4.71) is completed by the boundary conditions:

$$a_1(0, \eta) = \alpha_1(\eta), \qquad a_2(\xi, 0) = 0, \tag{4.73}$$

since the wave vectors $\mathbf{k}_{1,2}$ are orthogonal to the coordinates (ξ, η). The linear dispersion relation $\Omega = \Omega(K_\xi, K_\eta)$, where (K_ξ, K_η) are Fourier wave numbers, is given explicitly as

$$\left(\Omega - \frac{K_\xi + K_\eta}{2}\right)^2 = \alpha^2 + \left(\frac{K_\xi - K_\eta}{2}\right)^2. \tag{4.74}$$

Two surfaces of the dispersion relation for the two oblique waves are shown on Fig. 5 for $\alpha = 1$. Although the stop band is not the band gap in the characteristic coordinates (ξ, η), there exists a reference frame on the plane (ξ, η) that moves stationary in time T, where the stop band becomes the band gap of the dispersion relation (4.74). We set $\Omega = 0$ for simplicity and consider the Fourier transform solutions of the system (4.70)–(4.71):

$$a_1(\xi, \eta) = \int_{-\infty}^{\infty} kc(k) e^{i\alpha(k^{-1}\xi + k\eta)} dk, \tag{4.75}$$

$$a_2(\xi, \eta) = \int_{-\infty}^{\infty} c(k) e^{i\alpha(k^{-1}\xi + k\eta)} dk. \tag{4.76}$$

It follows from the boundary conditions (4.73) that $kc(k)$ is the Fourier transform of $\alpha_1(\eta/\alpha)$, subject to the following constraint:

$$0 = \int_{-\infty}^{\infty} c(k) e^{i\alpha k^{-1}\xi} dk, \qquad 0 \leq \xi \leq L_\xi. \tag{4.77}$$

Using the inverse Fourier transform,

$$kc(k) = \frac{\alpha}{2\pi} \int_0^{L_\eta} \alpha_1(\eta) e^{-i\alpha k\eta} d\eta, \tag{4.78}$$

and interchanging integrals, we reduce the constraint (4.77) to the form:

$$0 = \frac{\alpha}{2\pi i} \int_0^{L_\eta} \alpha_1(\eta) \left(\int_{-\infty}^{\infty} \frac{\sin \alpha(k\eta - k^{-1}\xi)}{k} dk \right) d\eta, \qquad 0 \leq \xi \geq L_\xi. \tag{4.79}$$

The inner integral is zero for $\xi > 0$ and $\eta > 0$, due to the table integral 3.871 on p. 474 of [9]. Therefore, the constraint (4.77) is satisfied and a unique solution of the problem (4.70)–(4.71) with (4.73) exists in the form (4.75)–(4.76) with (4.78).

We illustrate the Fourier transform solution (4.75)–(4.76) with the constant input function:

$$\alpha_1(\eta) = \alpha_1, \qquad \eta \in [0, L_\eta], \tag{4.80}$$

when $c(k)$ can be found explicitly as:

$$c(k) = \frac{\alpha_1}{2\pi i} \frac{1 - e^{-i\alpha k L_\eta}}{k^2}, \qquad k \in \mathbb{R}. \tag{4.81}$$

Evaluating Fourier integrals (4.75)–(4.76) with the help of the table integral 3.871 in [9], we find the explicit solution of the stationary problem:

$$a_1(\xi,\eta) = \alpha_1 J_0(2\alpha\sqrt{\xi\eta}), \qquad a_2(\xi,\eta) = \frac{i\alpha_1\sqrt{\eta}}{\sqrt{\xi}} J_1(2\alpha\sqrt{\xi\eta}), \tag{4.82}$$

where $J_{0,1}(z)$ are Bessel functions [9]. Figures 6(a,b) show the solution surfaces (4.82) for $|a_1(\xi,\eta)|^2$ and $|a_2(\xi,\eta)|^2$ in the domain (4.21) for $\alpha = 1$, $L_\xi = L_\eta = 10$, and $\alpha_1 = 1$. The integral invariants for the stationary transmission follow from integration of the balance equation:

$$\frac{\partial}{\partial\xi}|a_1|^2 + \frac{\partial}{\partial\eta}|a_2|^2 = 0. \tag{4.83}$$

We define the incident ($\mathcal{I}_{\text{in}}$), transmitted ($\mathcal{I}_{\text{out}}$), and diffracted ($\mathcal{I}_{\text{dif}}$) intensities by

$$\mathcal{I}_{\text{in}} = \int_0^{L_\eta} |a_1(0,\eta)|^2 d\eta, \quad \mathcal{I}_{\text{out}} = \int_0^{L_\eta} |a_1(L_\xi,\eta)|^2 d\eta, \quad \mathcal{I}_{\text{dif}} = \int_0^{L_\xi} |a_2(\xi,L_\eta)|^2 d\xi. \tag{4.84}$$

The transmittance (T) and diffractance (D) are defined by the same relations (4.61), such that the balance identity $T + D = 1$ follows from integration of the balance equation (4.83). The numerical values for T and D are found from numerical integration of the solution surfaces (4.84) as follows:

$$T \approx 0.032, \qquad D \approx 0.968,$$

such that $T + D \approx 1$. These values show that the incident wave is diffracted in the oblique resonance wave, such that only 3.2% of the wave energy remains in the transmitted wave.

5 Summary

We have shown that the coupled-mode equations can be used for analysis and modelling of resonant interaction of Bloch waves in low-contrast, weakly-nonlinear three-dimensional photonic crystals. The analytical solutions for stationary transmission problem can be found in the linear coupled-mode equations with the method of separation of variables and generalized Fourier series. We have proved that the stationary boundary-value problem is well-posed in the linear coupled-mode equations, in the context of two and four counter-propagating waves, as well as two oblique waves on the plane.

It is a further open problem to prove that the nonlinear stationary boundary-value problem is well-posed at least for small-norm solutions. Non-stationary transmission problems are also of interests, and very few analytical results are available on local and global well-posedness of the non-stationary coupled-mode equations. Finally, numerical approximations of the stationary and non-stationary, fully-nonlinear coupled-mode equations can be constructed in bounded

domains with the method of orthogonal polynomials [15, 16], which also contribute to the set of open problems, beyond the scopes of the present work.

Acknowledgements: The author thanks Dmitri Agueev, Ted Sargent, and Jamin Sheriff for collaboration and useful discussions. This paper has been completed during the author's visit to Universidad Autonoma del Estado de Mexico, organized and hosted by Dr. M. Aguero Granados.

A Explicit nonlinear functions for the system (3.13)–(3.16)

The cubic nonlinear functions $F_\pm$ and $G_\pm$ in the coupled-mode equations (3.13)–(3.16) for the four counter-propagating waves are listed here for future references:

$$\begin{aligned}
F_+ &= \beta_{0,0,0}\left((|A_+|^2+2|A_-|^2+2|B_+|^2+2|B_-|^2)A_+ + 2\bar{A}_- B_+ B_-\right) + \beta_{0,-1,0}\left(A_+^2\bar{B}_+ + 2A_+\bar{A}_- B_-\right)\\
&+ \beta_{1,1,0}\left((2|A_+|^2+|A_-|^2+2|B_+|^2+2|B_-|^2)A_- + 2\bar{A}_+ B_+ B_-\right) + \beta_{-1,0,0}\left(A_+^2\bar{B}_- + 2A_+\bar{A}_- B_+\right)\\
&+ \beta_{0,1,0}\left((2|A_+|^2+2|A_-|^2+|B_+|^2+2|B_-|^2)B_+ + 2A_+A_-\bar{B}_-\right) + \beta_{-1,1,0}\left(2A_+B_+\bar{B}_- + \bar{A}_- B_+^2\right)\\
&+ \beta_{1,0,0}\left((2|A_+|^2+2|A_-|^2+2|B_+|^2+|B_-|^2)B_- + 2A_+A_-\bar{B}_+\right) + \beta_{1,-1,0}\left(2A_+\bar{B}_+B_- + \bar{A}_- B_-^2\right)\\
&+ \beta_{2,0,0}\left(\bar{A}_+ B_-^2 + 2A_-\bar{B}_+B_-\right) + \beta_{2,1,0}\left(2\bar{A}_+A_-B_- + A_-^2\bar{B}_+\right) + \beta_{1,2,0}\left(A_-^2\bar{B}_- + 2\bar{A}_+A_-B_+\right)\\
&+ \beta_{0,2,0}\left(\bar{A}_+B_+^2 + 2A_-B_+\bar{B}_-\right) + \beta_{-1,-1,0}A_+^2\bar{A}_- + \beta_{2,2,0}\bar{A}_+A_-^2 + \beta_{2,-1,0}\bar{B}_+B_-^2 + \beta_{-1,2,0}B_+^2\bar{B}_-,
\end{aligned}$$

$$\begin{aligned}
F_- &= \beta_{-1,-1,0}\left((|A_+|^2+2|A_-|^2+2|B_+|^2+2|B_-|^2)A_+ + 2\bar{A}_- B_+ B_-\right) + \beta_{-1,-2,0}\left(A_+^2\bar{B}_+ + 2A_+\bar{A}_- B_-\right)\\
&+ \beta_{0,0,0}\left((2|A_+|^2+|A_-|^2+2|B_+|^2+2|B_-|^2)A_- + 2\bar{A}_+ B_+ B_-\right) + \beta_{-2,-1,0}\left(A_+^2\bar{B}_- + 2A_+\bar{A}_- B_+\right)\\
&+ \beta_{-1,0,0}\left((2|A_+|^2+2|A_-|^2+|B_+|^2+2|B_-|^2)B_+ + 2A_+A_-\bar{B}_-\right) + \beta_{-2,0,0}\left(2A_+B_+\bar{B}_- + \bar{A}_- B_+^2\right)\\
&+ \beta_{0,-1,0}\left((2|A_+|^2+2|A_-|^2+2|B_+|^2+|B_-|^2)B_- + 2A_+A_-\bar{B}_+\right) + \beta_{0,-2,0}\left(2A_+\bar{B}_+B_- + \bar{A}_- B_-^2\right)\\
&+ \beta_{1,-1,0}\left(\bar{A}_+ B_-^2 + 2A_-\bar{B}_+B_-\right) + \beta_{1,0,0}\left(2\bar{A}_+A_-B_- + A_-^2\bar{B}_+\right) + \beta_{0,1,0}\left(A_-^2\bar{B}_- + 2\bar{A}_+A_-B_+\right)\\
&+ \beta_{-1,1,0}\left(\bar{A}_+B_+^2 + 2A_-B_+\bar{B}_-\right) + \beta_{-2,-2,0}A_+^2\bar{A}_- + \beta_{1,1,0}\bar{A}_+A_-^2 + \beta_{1,-2,0}\bar{B}_+B_-^2 + \beta_{-2,1,0}B_+^2\bar{B}_-,
\end{aligned}$$

$$\begin{aligned}
G_+ &= \beta_{0,-1,0}\left((|A_+|^2+2|A_-|^2+2|B_+|^2+2|B_-|^2)A_+ + 2\bar{A}_- B_+ B_-\right) + \beta_{0,-2,0}\left(A_+^2\bar{B}_+ + 2A_+\bar{A}_- B_-\right)\\
&+ \beta_{1,0,0}\left((2|A_+|^2+|A_-|^2+2|B_+|^2+2|B_-|^2)A_- + 2\bar{A}_+ B_+ B_-\right) + \beta_{-1,-1,0}\left(A_+^2\bar{B}_- + 2A_+\bar{A}_- B_+\right)\\
&+ \beta_{0,0,0}\left((2|A_+|^2+2|A_-|^2+|B_+|^2+2|B_-|^2)B_+ + 2A_+A_-\bar{B}_-\right) + \beta_{-1,0,0}\left(2A_+B_+\bar{B}_- + \bar{A}_- B_+^2\right)\\
&+ \beta_{1,-1,0}\left((2|A_+|^2+2|A_-|^2+2|B_+|^2+|B_-|^2)B_- + 2A_+A_-\bar{B}_+\right) + \beta_{1,-2,0}\left(2A_+\bar{B}_+B_- + \bar{A}_- B_-^2\right)\\
&+ \beta_{2,-1,0}\left(\bar{A}_+ B_-^2 + 2A_-\bar{B}_+B_-\right) + \beta_{2,0,0}\left(2\bar{A}_+A_-B_- + A_-^2\bar{B}_+\right) + \beta_{1,1,0}\left(A_-^2\bar{B}_- + 2\bar{A}_+A_-B_+\right)\\
&+ \beta_{0,1,0}\left(\bar{A}_+B_+^2 + 2A_-B_+\bar{B}_-\right) + \beta_{-1,-2,0}A_+^2\bar{A}_- + \beta_{2,1,0}\bar{A}_+A_-^2 + \beta_{2,-2,0}\bar{B}_+B_-^2 + \beta_{-1,1,0}B_+^2\bar{B}_-,
\end{aligned}$$

$$\begin{aligned}
G_- &= \beta_{-1,0,0}\left((|A_+|^2+2|A_-|^2+2|B_+|^2+2|B_-|^2)A_+ + 2\bar{A}_- B_+ B_-\right) + \beta_{-1,-1,0}\left(A_+^2\bar{B}_+ + 2A_+\bar{A}_- B_-\right)\\
&+ \beta_{0,1,0}\left((2|A_+|^2+|A_-|^2+2|B_+|^2+2|B_-|^2)A_- + 2\bar{A}_+ B_+ B_-\right) + \beta_{-2,0,0}\left(A_+^2\bar{B}_- + 2A_+\bar{A}_- B_+\right)
\end{aligned}$$

$$+ \quad \beta_{-1,1,0}\left((2|A_+|^2+2|A_-|^2+|B_+|^2+2|B_-|^2)B_+ + 2A_+A_-\bar{B}_-\right) + \beta_{-2,1,0}\left(2A_+B_+\bar{B}_- + \bar{A}_-B_+^2\right)$$
$$+ \quad \beta_{0,0,0}\left((2|A_+|^2+2|A_-|^2+2|B_+|^2+|B_-|^2)B_- + 2A_+A_-\bar{B}_+\right) + \beta_{0,-1,0}\left(2A_+\bar{B}_+B_- + \bar{A}_-B_-^2\right)$$
$$+ \quad \beta_{1,0,0}\left(\bar{A}_+B_-^2 + 2A_-\bar{B}_+B_-\right) + \beta_{1,1,0}\left(2\bar{A}_+A_-B_- + A_-^2\bar{B}_+\right) + \beta_{0,2,0}\left(A_-^2\bar{B}_- + 2\bar{A}_+A_-B_+\right)$$
$$+ \quad \beta_{-1,2,0}\left(\bar{A}_+B_+^2 + 2A_-B_+\bar{B}_-\right) + \beta_{-2,-1,0}A_+^2\bar{A}_- + \beta_{1,2,0}\bar{A}_+A_-^2 + \beta_{1,-1,0}\bar{B}_+B_-^2 + \beta_{-2,2,0}B_+^2\bar{B}_-.$$

References

[1] N. Akozbek and S. John, "Optical solitary waves in two- and three-dimensional nonlinear photonic band-gap structures", Phys. Rev. E **57**, 2287–2319 (1998).

[2] N. Akozbek and S. John, "Self-induced transparency solitary waves in a doped nonlinear photonic band gap materials", Phys. Rev. E **58**, 3876–3895 (1998).

[3] A. Arraf and C.M. de Sterke, "Coupled-mode equations for quadratically nonlinear deep gratings", Phys. Rev. E **58**, 7951–7958 (1998).

[4] A. Babin and A. Figotin, "Nonlinear photonic crystals: I. Quadratic nonlinearity", Waves in Random Media **11**, R31–R102 (2001).

[5] A. Babin and A. Figotin, "Nonlinear photonic crystals: II. Interaction classification for quadratic nonlinearities", Waves in Random Media **12**, R25–R52 (2002).

[6] N. Bhat and J.E. Sipe, "Optical pulse propagation in nonlinear photonic crystals", Phys. Rev. E **64**, 056604 (2001)

[7] E.A. Coddington and N. Levinson, "*Theory of Ordinary Differential Equations*", (McGraw-Hill, New York, 1955).

[8] R.H. Goodman, M.I. Weinstein, and P.J. Holmes, "Nonlinear propagation of light in one-dimensional periodic structures", J. Nonlin. Science **11**, 123–168 (2001).

[9] I.S. Gradshtein, I.M. Ryzhik, *Table of integrals, series, and products* (Academic Press, 2000).

[10] C. Kittel, *Introduction to Solid–State Physics* (John Wiley & Sons, 1996).

[11] P.Kuchment, *Floquet Theory for Partial Differential Operators* (Birkhauser, Basel, 1993).

[12] P. Kuchment, "The mathematics of photonic crystals", in *Mathematical Modeling in Optical Sciences* (SIAM, Philadelphia, 1999).

[13] D. Pelinovsky, J. Sears, L. Brzozowski, and E.H. Sargent, "Stable all-optical limiting in nonlinear periodic structures. I: Analysis", J. Opt. Soc. Am. B **19**, 43–53 (2002).

[14] D.E. Pelinovsky and A. Scheel, "Spectral analysis of stationary light transmission in nonlinear photonic structures", J. Nonlin. Science, **13**, 347-396 (2003).

[15] J. Shen, "Efficient spectral-Galerkin method I: Direct solvers of second-order and fourth-order equations using Legendre polynomials", SIAM J. Sci. Comput. **15**, 1489–1505 (1994).

[16] J. Shen and L.L. Wang, "Legendre and Chebyshev dual-Petrov-Galerkin methods for hyperbolic equations", AMS Math. & Comp., to be published (2004).

[17] J.L. Sheriff, I.A. Goldthorpe, and E.H. Sargent, "Optical limiting and intensity-dependent diffraction from low-contrast nonlinear periodic media: coupled-mode analysis", Phys. Rev. E, to be published (2004).

[18] C.M. de Sterke and J.E. Sipe, "Envelope-function approach for the electrodynamics of nonlinear periodic structures", Phys. Rev. A **38**, 5149–5165 (1988).

[19] C.M. de Sterke and J.E. Sipe, "Extensions and generalizations of an envelope-function approach for the electrodynamics of nonlinear periodic structures", Phys. Rev. A **39**, 5163–5178 (1989).

[20] C.M. de Sterke, D.G. Salinas, and J.E. Sipe, "Coupled-mode theory for light propagation through deep nonlinear gratings", Phys. Rev. E **54**, 1969–1989 (1996).

[21] C.M. de Sterke and J.E. Sipe, "Gap solitons", Progress in Optics, **33**, 203 (1994).

[22] W. Strauss, "*Partial Differential Equations: an Introduction*", (Wiley & Sons, New York, 1992).

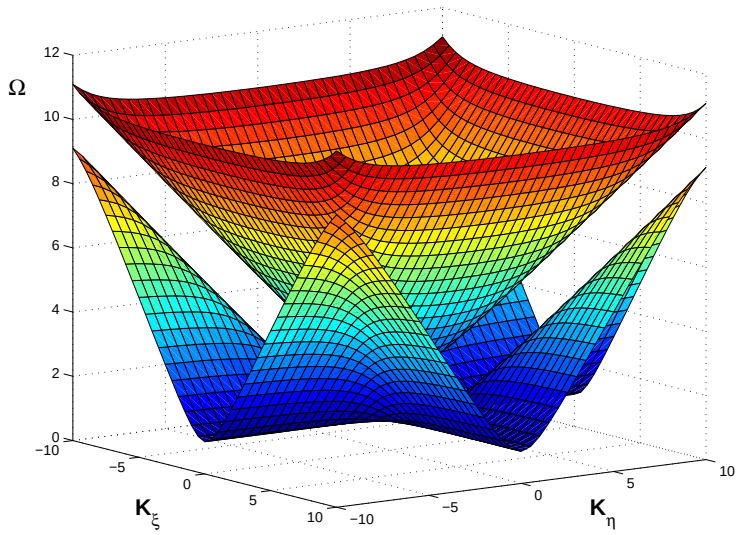

Figure 1: Dispersion relations $\Omega = \Omega(K_\xi, K_\eta)$ from the roots of the determinant equation (4.23) for $\alpha = 1$, $\beta = i$, and $\Omega > 0$.

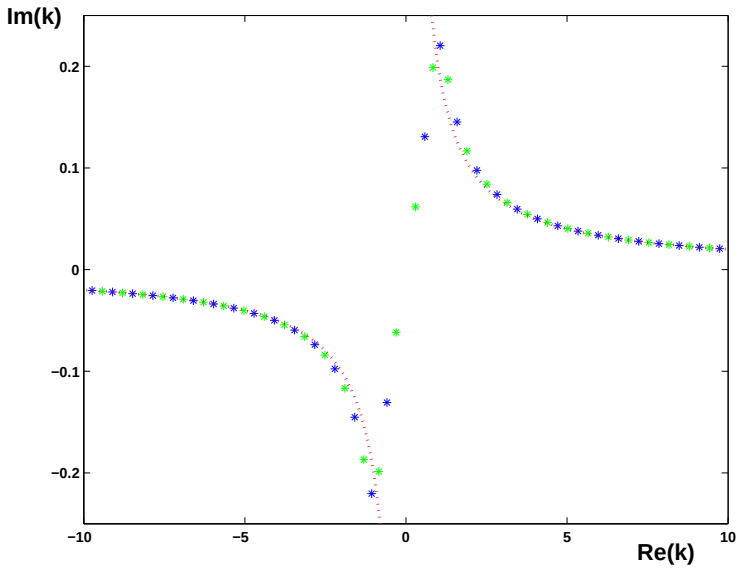

Figure 2: Roots $k \in \mathcal{R}$ and $(-k) \in \mathcal{R}$ of the characteristic equation (4.36) for $\alpha = 1$ and $L_\eta = 10$. The dotted curves show the leading-order asymptotic approximation (4.40).

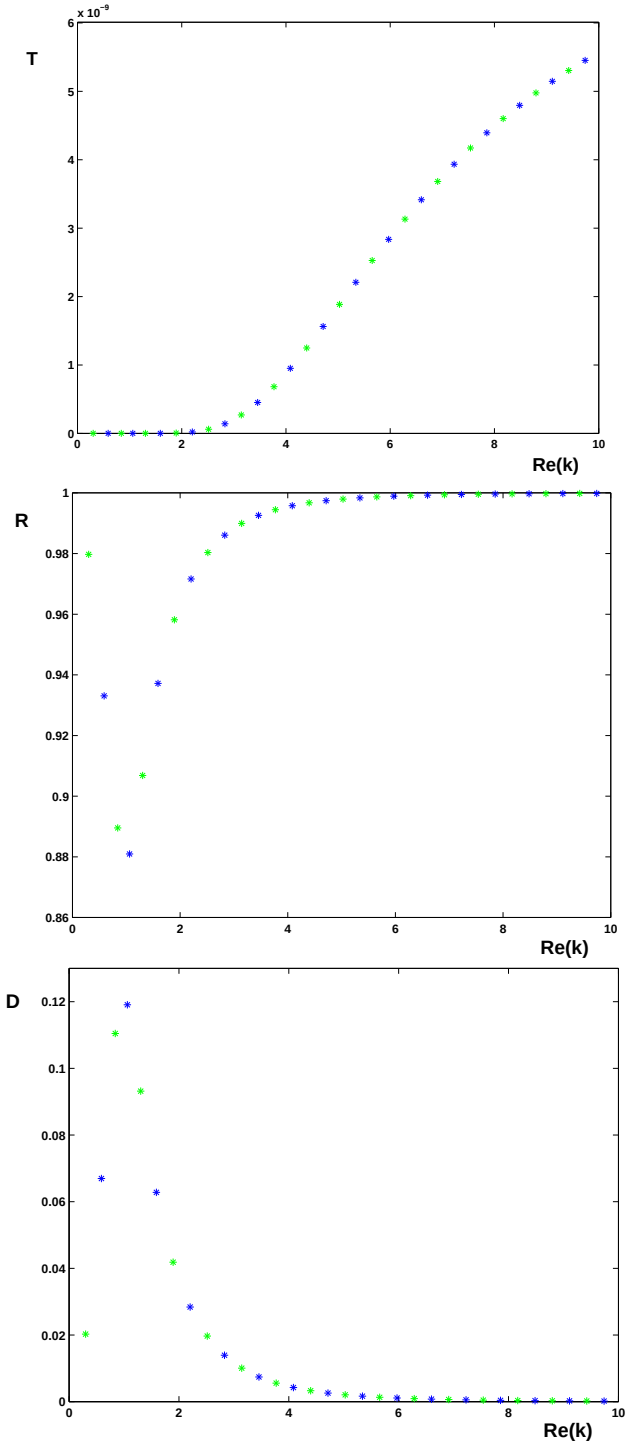

Figure 3: Transmittance (T), reflectance (R), and diffractance (D) versus $\mathrm{Re}(k)$ for the roots $k \in \mathcal{R}$, when $\alpha = 1$, $\beta = i$, and $L_\xi = L_\eta = 10$.

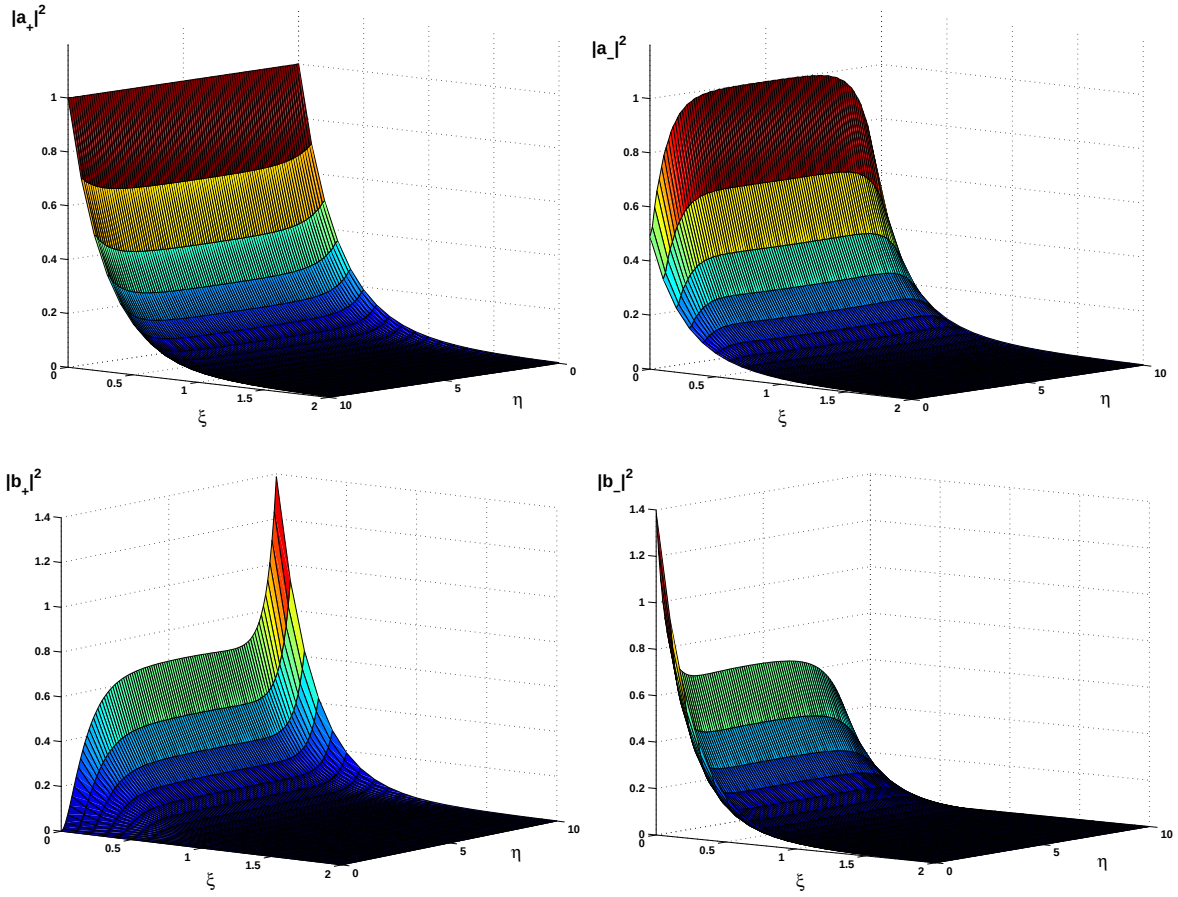

Figure 4: Solution surfaces $|a_{\pm}|^2$ and $|b_{\pm}|^2$ on the domain $\mathcal{D}$ for $\alpha = 1$, $\beta = i$, $L_\xi = L_\eta = 10$, and $\alpha_+ = 1$.

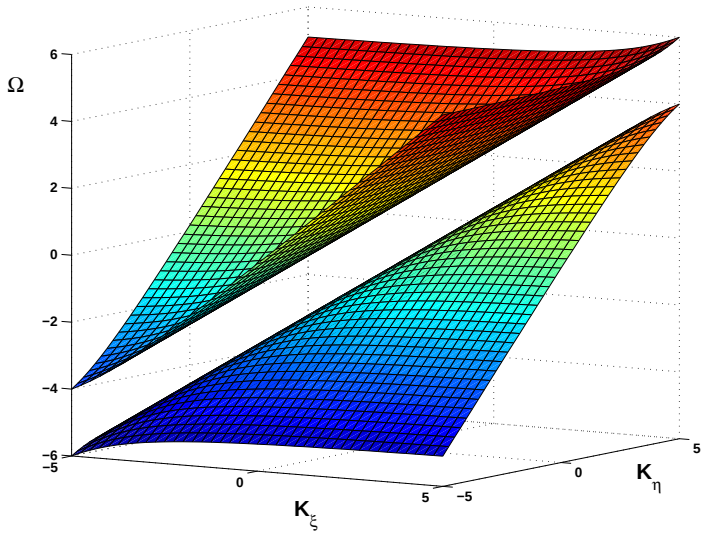

Figure 5: Dispersion relations $\Omega = \Omega(K_\xi, K_\eta)$ from the dispersion equation (4.74) for $\alpha = 1$.

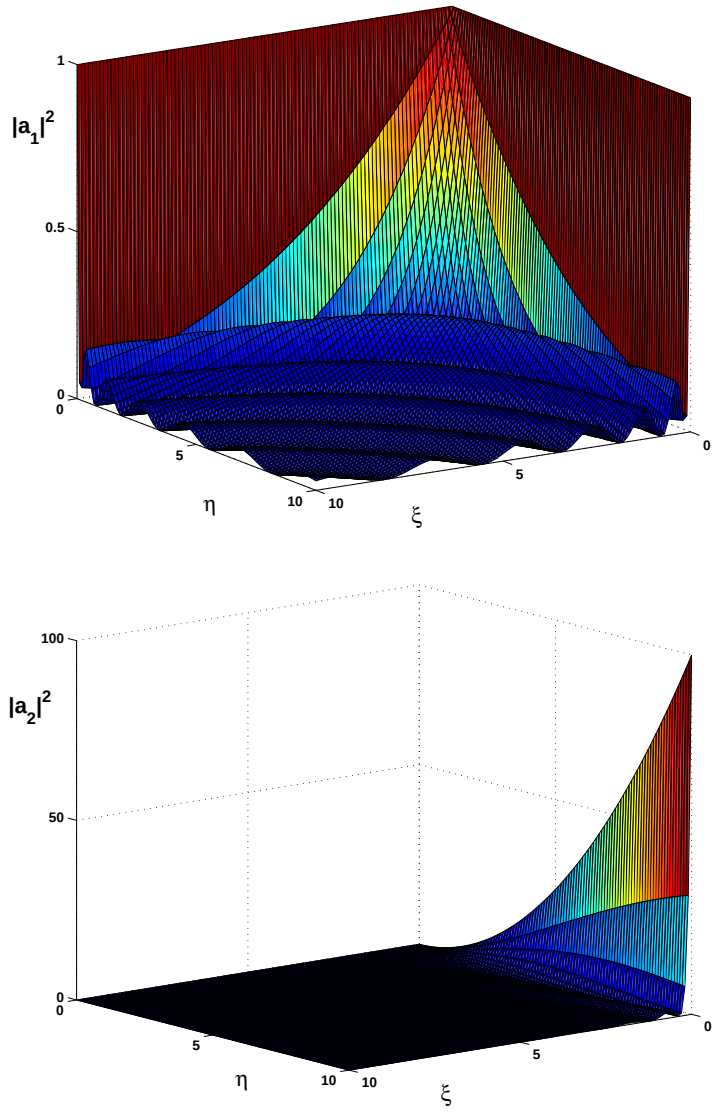

Figure 6: Solution surfaces $|a_1|^2$ and $|a_2|^2$ on the domain $\mathcal{D}$ for $\alpha = 1$, $L_\xi = L_\eta = 10$, and $\alpha_1 = 1$.